Adult *Hox* gene expression promotes periosteal stem cell maintenance and mediates reprogramming in a regionally restricted manner

Authors: Kevin Leclerc[1], Lindsey H. Remark[1,2], Malissa Ramsukh[1], Anne Marie Josephson[1,2], Sophie M. Morgani[1], Laura Palma[1], Paulo EL Parente[1], Sooyeon Lee[3], Emma Muiños Lopez[4], Philipp Leucht[1,2]

Affiliations

[1] Department of Orthopaedic Surgery, NYU Robert I. Grossman School of Medicine, New York, NY, United States of America
[2] Department of Cell Biology, NYU Robert I. Grossman School of Medicine, New York, NY, United States of America
[3] Institute of Comparative Molecular Endocrinology, Ulm University, Ulm, Germany
[4] Cell Therapy Area, Clínica Universidad de Navarra, Pamplona, Spain.

Corresponding Author: Philipp Leucht – Email: philipp.leucht@nyulangone.org

Abstract

Periosteal stem and progenitor cells are pivotal to the growth and lifelong turnover of bone and underpin its capacity to regenerate. Adjusting the potency of this cell population will therefore be critical to the successful generation and application of new bone repair therapies. Following their role in patterning the embryonic skeleton, *Hox* genes remain regionally expressed in mesenchymal stromal cell populations of the adult skeleton. Here we show that *Hoxa10* is most expressed in the most uncommitted periosteal stem cell and that *Hox* maintains these skeletal stem cells in a multipotential, uncommitted state, thereby preventing their differentiation into bone. We demonstrate that *Hoxa10* mediates the reprogramming of periosteal progenitors towards a stem cell state with greater self-renewal capacity and also establish that region-specific *Hox* genes mediate cell reprogramming in distinct anatomical regions, demonstrating the continued functional relevance of the embryonic *Hox* profile in adult stem cells. Together, our data describe a master regulator

role of *Hox* in skeletal stem and progenitor cells and help provide insight into the development of cell-based therapies for treatment of at-risk bone fractures and other bone-related ailments.

Introduction

Bone homeostasis and repair is mediated by skeletal stem cells (SSCs) that self-renew and differentiate into the major skeletal/mesenchymal lineages (stromal, osteo-, chondro-, and adipo-lineages) (Zhou, Yue et al. 2014, Yue, Zhou et al. 2016, Ambrosi, Longaker et al. 2019). SSCs harbor massive therapeutic potential as an unlimited source of differentiated cells to replace those lost and damaged in injury and disease. However, during aging, they are relatively rare and the molecular and genetic mechanisms that regulate stem cell number and function are still largely unknown.

Skeletal stem and progenitor cells reside in the bone marrow of long bones, and also on the inner and outer surfaces of cortical bone. It was recently shown that the periosteum, a layer of mesenchymal cells that lines the outer cortex of the bone, is highly enriched for SSCs that are transcriptionally distinct from stem cells from other regions (Duchamp de Lageneste, Julien et al. 2018). Although periosteal cells have higher regenerative capacity than mesenchymal cells derived from bone marrow, they remain poorly characterized. Recent evidence suggests that periosteal stem and progenitor cells (PSPCs) are the main contributor to the fracture callus after long bone fractures (Colnot, Zhang et al. 2012, Ferretti and Mattioli-Belmonte 2014, Roberts, van Gastel et al. 2015, Duchamp de Lageneste, Julien et al. 2018), pinpointing this population as an important therapeutic target to improve fracture healing in patients that are prone to developing a nonunion – such as aged patients (Nilsson and Edwards 1969, Nieminen, Nurmi et al. 1981, Gruber, Koch et al. 2006, Kwong and Harris 2008) or patients with high-energy injuries and accompanying soft tissue loss (Harris, Althausen et al. 2009, Cheng, Vantucci et al. 2021).

Homeobox (Hox) genes are evolutionarily conserved transcription factors that are master regulators of positional identity and cell fate specification during embryonic development (Deschamps and van Nes 2005). The mouse and human genomes contain 39 *Hox* genes, which are grouped into four clusters, *Hoxa*, *Hoxb*, *Hoxc*, and *Hoxd*, positioned on four separate chromosomes in 13 paralogs (Izpisua-Belmonte, Falkenstein et al. 1991, Krumlauf 1994). During development, overlapping patterns of *Hox* gene activity assign a segmental identity to each anatomic body part, which culminates in the creation of a complex tissue, organ or organism. While this genetic blueprint is essential to establish the body plan of an organism, its function in adulthood is unclear. *Hox* genes are expressed during homeostasis and tissue repair (Pineault, Helgason et al. 2002, Leucht, Kim et al. 2008, Gerber, Murawala et al. 2018, Bradaschia-Correa, Leclerc et al. 2019, Lin, Gerber et al. 2021), suggesting that the Hox code may also be required for successful regeneration and could similarly impart positional information and, in skeletal tissues, *Hoxa11*-expressing cells comprise a stem/progenitor cell population necessary for successful fracture healing of the ulna (Rux, Song et al. 2016, Song, Pineault et al. 2020). However, the precise function of *Hox* genes in adulthood is yet unknown and, surprisingly, little is known regarding the regional specificity of adult *Hox* gene function.

Here we identify *Hox* genes as key regulators of skeletal stem cell maintenance. We show that *Hox* deficiency leads to a decrease in stem cell number and proliferation, and an increase in their propensity to undergo spontaneous differentiation toward osteogenic, adipogenic, and chondrogenic fates. Conversely, an increase in *Hoxa10* expression reduces PSPC differentiation potential and increases the self-renewal capacity of the stem cell compartment. During differentiation, SSCs give rise to a larger number of fate-restricted progenitors that have limited lineage potential and lifespan (Chan, Seo et al. 2015, Debnath, Yallowitz et al. 2018). Here, we also uncover the ability of *Hox* genes to drive periosteal progenitor reprogramming to a more uncommitted bona fide stem cell state and further establish that the reprogramming capacity of specific *Hox* genes is restricted to the anatomical regions that reflect their embryonic expression pattern. Harvesting and reprogramming more prevalent progenitor populations may represent an innovative source of SSCs and a promising strategy to combat bone deficiencies, such as the aged-associated

bone loss driven by a decline in SSC number and function (Josephson, Bradaschia-Correa et al. 2019).

Results

Hox gene expression is enriched in skeletal stem/ progenitor cells and declines with age

Hox genes regulate morphogenesis and regeneration in multiple organisms (Gardiner and Bryant 1996, Orii, Kato et al. 1999, Nogi and Watanabe 2001, Christen, Beck et al. 2003, Thummel, Ju et al. 2007). In several vertebrate organs, *Hox* gene expression marks subpopulations of mesenchymal stem cells (Hwang, Seok et al. 2009, Liedtke, Buchheiser et al. 2010, Rux, Song et al. 2016, Bradaschia-Correa, Leclerc et al. 2019) that mediate tissue repair. To investigate the role of *Hox* genes within the adult skeleton, we first analyzed their expression within LEPR$^+$ skeletal stem and progenitor cells (SSPCs) and the microenvironment – comprising differentiated skeletal lineages, CD45$^+$ hematopoietic, CD31$^+$ erythroid, and TER119$^+$ endothelial cells – using our previously generated RNA-sequencing dataset of hindlimb skeletal elements (Josephson, Bradaschia-Correa et al. 2019). Previous reports showed that *Hoxa11* marks a population of bone marrow stem cells (Rux, Song et al. 2016). Our analysis revealed that all Hox family members are enriched in SSPCs relative to the microenvironment (**Fig. 1A)**, suggesting that they play a crucial role in stem cell function. Specifically, *Hoxa10* was most highly expressed and enriched 50-fold in skeletal stem cells compared to cells of the microenvironment ($p = 0.0043$). SSPC number and function decline with age (Josephson, Bradaschia-Correa et al. 2019, Ambrosi, Marecic et al. 2021), leading to a reduction in the regenerative capacity of bone. Intriguingly, using our RNA sequencing dataset (Josephson, Bradaschia-Correa et al. 2019), we noted that the majority of *Hox* genes were downregulated in LEPR$^+$ SSPCs harvested from the hindlimbs of middle-aged (52-week-old) mice when compared to those of young (12-week-old) (**Fig. 1B**). This result was confirmed in bone marrow samples harvested from the fracture sites of young (19-39 years-old) and aged (61-86 years-old) human patients (including 7 males and 8 females) where the older cohort of patients displayed about half of the *Hoxa10* levels expressed by the younger cohort by qRT-PCR (**Fig. 1C**). We further corroborated these data

in the periosteal compartment of aged mice, which show a large reduction in the frequency of CD49f^{low}CD51^{low}:CD200^{+}CD105^{-} periosteal stem cells as defined by *Debnath et al.* (Debnath, Yallowitz et al. 2018) (**Fig. 1D**) and display significantly less *Hoxa10* expression by qRT-PCR when compared to young mice (**Fig. 1E**). Altogether these data indicate that *Hox* expression is associated with functional skeletal stem cells.

Hoxa10 is the most highly expressed Hox gene in tibial periosteal cells

Hox gene clusters display spatial collinearity, an increase in the expression of sequential *Hox* genes as development proceeds along the anterior-posterior (A-P) axis. Several *Hox* genes are co-activated at a given position along the A-P axis with the most highly expressed representing the key regulator within that region (Izpisua-Belmonte, Falkenstein et al. 1991, Papageorgiou 2012, Darbellay, Bochaton et al. 2019). We, therefore, hypothesized that *Hox* expression in adult tissues correlates with essential functions. To quantify *Hox* gene expression in skeletal stem cells and progenitors during homeostasis and assess whether this recapitulates the embryonic pattern, we performed bulk RNA sequencing and Nanostring nCounter® gene expression technology on cells isolated from adult tibiae. While numerous skeletal stem cell populations have been described (Costa, Eiro et al. 2021, Mabuchi, Okawara et al. 2021), we chose to focus here on periosteal stem cells as they demonstrate the highest regenerative capacity (Colnot, Zhang et al. 2012, Ferretti and Mattioli-Belmonte 2014, Roberts, van Gastel et al. 2015, Duchamp de Lageneste, Julien et al. 2018). Both analyses indicated that *Hoxa10* is the most highly expressed family member in the adult tibial periosteum (**Fig. 2A, Supplementary Fig. 1A, B**). To conduct a more detailed analysis of *Hoxa10*'s expression pattern within the periosteal compartment, we next separated periosteal cells into periosteal stem cells (PSC) (CD49f^{low}CD51^{low}:CD200^{+}CD105^{-}), periosteal progenitor 1 cells (PP1) (CD49f^{low}CD51^{low}:CD200^{-}CD105^{-}) and periosteal progenitor 2 cells (PP2) (CD49f^{low}CD51^{low}:CD105^{+}CD200^{variable}) using flow cytometry, according to *Debnath et al*. (Debnath, Yallowitz et al. 2018) (**Fig. 2B, C, and Supplementary Fig. 1C**). Using qRT-PCR, we observed high *Hoxa10* expression in PSCs, the most uncommitted compartment, and lower expression in PP1 and PP2 cells (**Fig. 2D**), which are more lineage-restricted (Debnath, Yallowitz et al. 2018). This is consistent with studies in the hematopoietic system,

endometrium, and craniofacial skeleton, which show that *Hoxa10* is expressed by adult cells with high plasticity (Kanzler, Kuschert et al. 1998, Creuzet, Couly et al. 2002, Magnusson, Brun et al. 2007, Zanatta, Rocha et al. 2010).

Hoxa10 is among the first genes to be downregulated at the initiation of differentiation

Stem cell differentiation is often a two-step process that involves first dismantling the gene regulatory network that maintains self-renewal before subsequently upregulating a lineage-specific transcriptional program (Bardin, Perdigoto et al. 2010, Kalkan, Olova et al. 2017). As *Hox* genes are highly enriched in SSPCs (**Fig. 1A**) , we hypothesize that they maintain skeletal progenitors in an undifferentiated state. In support of this, in the adult zeugopod, *Hoxa11* is expressed in skeletal stem cells marked by, PDGFRα and CD51, and is absent from differentiated Osterix^{+} osteoblasts, Sox9^{+} chondrocytes, and Perilipin^{+} adipocytes (Rux, Song et al. 2016). However, comparatively little is known about *Hox* expression dynamics in the intermediate steps as cells transition from stem cells and start the differentiation process. If *Hoxa10* maintains cells in a primitive stem cell state, then one would expect its expression to be promptly shutdown when cells are challenged to differentiate. As PSCs are extremely rare, to investigate this we isolated PP1 early progenitor cells from the tibia by fluorescence activated cell sorting (FACS) and analyzed dynamic gene expression changes over the first 18 hours of osteogenic or adipogenic differentiation. Under both conditions, *Hoxa10* was rapidly downregulated by 2 hours of differentiation, even before known stem cell-associated genes (such as *Pdgfrα* and *CyclinD1*) were downregulated and lineage markers (like *FosB* and *Runx2*) were upregulated (**Fig. 2E, F**). These data suggest that *Hoxa10* must be downregulated for differentiation to proceed and underpins its potential role as a stem cell maintenance factor.

Inhibition of Hox genes in stem and progenitor cells triggers a loss of skeletal stem cells and periosteal stemness properties

We hypothesize that *Hox* expression functions in skeletal stem cells, and not in more committed cells, to maintain the stem cell pool. In knockdown/knockout experiments, the role of individual *Hox* genes is frequently masked by the functional redundancy of other family members (Carpenter, Goddard et al. 1993, Mark, Lufkin et al. 1993, Studer, Lumsden

et al. 1996, Gavalas, Studer et al. 1998, Rossel and Capecchi 1999, McNulty, Peres et al. 2005, Rux, Song et al. 2016, Song, Pineault et al. 2020). To test the maintenance role of *Hox* in the context of *in vivo* bone regeneration and to thwart potential redundancy of *Hox* genes, we utilized a conditional allele of the ~100kb span of the *HoxA* cluster (Kmita, Tarchini et al. 2005) and paired it to three separate Cre drivers, $Pdgfr\alpha^{CreERT}$, Osx^{CreERT}, and $Col1a1^{CreERT}$ that would target the *HoxA* family in increasingly more committed skeletal cells. Transgenic mice were given tamoxifen starting a week before tibial injury using a standardized tibial monocortical defect model, and EdU was also administered to the mice one day before sacrificing them to test proliferation capacity (**Fig. 3A**). Compared to control animals, knocking out the *HoxA* cluster in the $Pdgfr\alpha^{+}$ stem and progenitor domain (Morikawa, Mabuchi et al. 2009, Pinho, Lacombe et al. 2013, Ambrosi, Longaker et al. 2019) during tibial injury led to a large reduction of $6C3^{-}CD90^{-}CD51^{+}CD200^{+}CD105^{-}$ skeletal stem cells, a concomitant increase in the more committed $6C3^{-}CD90^{-}CD51^{+}CD200^{-}CD105^{-}$ pre-Bone/Chondro/Stromal progenitors (pre-BCSPs), and a significant loss of proliferative capacity when probing cells harvested from the injury site at 3 days post injury by flow cytometry (**Fig. 3B**). This suggests that there may be a cell state shift as cells lose stemness and accumulate in this more committed cell state. The deletion of *HoxA* in more committed Osx^{+} pre-osteoblasts (Mizoguchi, Pinho et al. 2014, Mabuchi, Okawara et al. 2021) resulted in a decrease in the pre-BCSP population without any change in proliferative activity (**Fig. 3C**). In contrast, *HoxA* deletion in $Col1a1^{+}$ mature osteoblasts (Kalajzic, Kalajzic et al. 2002) had no effect on skeletal stem and progenitor populations or proliferative capacity (**Fig. 3D**). Altogether, these results indicate that *Hox* genes are essential to the maintenance of skeletal stemness in the most primitive lineages present during skeletal regeneration.

To directly examine the role of *Hox* genes in periosteal stem and progenitor cells (PSPCs), we utilized an *si*RNA strategy to moderate their expression in isolated and cultured tibial periosteal cells, which are highly enriched for PSPCs (**Supplementary Fig. 1C, third panel**). To minimize potential redundancy between *Hox* genes highly expressed in these cells, we employed a mix of multiple siRNAs targeting *Hoxa10* and *11*, and *Hoxd10* and *11*, and *Hoxc10* (*HoxMix*), the most highly expressed *Hox* genes of the tibia periosteum. This strategy resulted in a significant reduction of the targeted *Hox* genes (**Supplementary Fig. 2A**). *Hoxa2*, a more proximal *Hox* gene, was not affected by the *HoxMix* siRNAs, confirming

the specificity of this approach (**Supplementary Fig. 2A**). After seven days, we then assessed the impact of *Hox* knockdown on the skeletal stem cell state by analyzing the expression of the conventional skeletal stem cell markers SCA1 and PDGFRα (Houlihan, Mabuchi et al. 2012, Rux, Song et al. 2016) by flow cytometry. We found that cell cultures treated with *HoxMix* siRNAs had a significantly smaller proportion of cells that expressed both SCA1 and PDGFRα, while the size of the SCA1^{-}/PDGFRα^{-} population increased, suggesting a shift from primitive undifferentiated to more mature, specified cells after *Hox* knockdown or priming towards more committed states (**Fig. 3E**).

Self-renewal and proliferation are hallmarks of stemness. The loss of *Hoxb4* and *Hoxa9* impairs proliferation and hinders the repopulating ability of hematopoietic stem cells (Bjornsson, Larsson et al. 2003, Brun, Bjornsson et al. 2004, Lawrence, Christensen et al. 2005). To determine whether a reduction in *Hox* genes also affects this functional property of skeletal stem cells, we performed an EdU incorporation assay on tibial periosteal cells after posterior *Hox* genes were downregulated using *HoxMix*. This demonstrated that proliferation and PSPC numbers decreased (**Fig. 3F**, **Supplementary Fig. 2D**), signifying the loss of stemness-associated characteristics. To investigate this further, we used CellTrace^{TM} to track cell cycle kinetics over multiple cell generations. In this assay cells were initially saturated with a fluorescent dye and, with each cell division, the dye is diluted in the daughter generation of cells. The amount of dye remaining in the cells after six days, as measured by flow cytometry, then revealed the generation number and cyling rate of cells assayed. Under control conditions, stem/progenitor cells predominantly comprise a higher-generation population of cells and are therefore high-cycling (**Supplementary Fig. 2B, C**). Following siRNA administration, generational analysis revealed that control cells continued to cycle and self-renew, with a large percentage being in the stemness-associated generation 7+, while *HoxMix* knockdown resulted in a reduction of cells in the higher generations (**Fig. 3G**), again supporting the hypothesis that *Hox* deficiency leads to a loss of stemness and lineage progression towards differentiation.

Downregulation or loss of genes associated with stemness can dismantle the self-renewal gene regulatory network and trigger aberrant spontaneous differentiation. For example, in the developing embryonic palate and other craniofacial skeletal elements, lack of *Hoxa2* induces an increase in differentiation and an upregulation of bone and cartilage markers

(Kanzler, Kuschert et al. 1998, Dobreva, Chahrour et al. 2006, Iyyanar and Nazarali 2017). To probe the effect of *Hox* deficiency on tibial periosteal cell differentiation propensity, serial siRNA transfections were employed to suppress *Hox* for 14 days. Gene expression analysis confirmed the continued repression of *Hox* genes, and downregulation of the stem cell marker, *Pdgfrα*, in periosteal cells transfected with *HoxMix* (**Supplementary Fig. 2E, F**) and, in the absence of overt differentiation cues, these cells showed an increase in the expression of a cohort of osteogenic, adipogenic, and chondrogenic markers when compared to those treated with control siRNA (**Fig. 3H**). Together, these results demonstrate that, a reduction of *Hox* expression in skeletal stem and progenitor cells results in a loss of self-renewal capacity and an increase in spontaneous tri-lineage differentiation.

Hoxa10 expression is sufficient to induce a skeletal stem cell state

The redundancy between *Hox* genes often obfuscates their function in loss-of-function experiments, hence the clearest indications for a role of HOX transcription factors in the regulation and maintenance of adult stem cells have come from overexpression studies (Sauvageau, Thorsteinsdottir et al. 1995, Lawrence, Sauvageau et al. 1996, Thorsteinsdottir, Sauvageau et al. 1997, Thorsteinsdottir, Mamo et al. 2002). As we found that *Hox* knockdown results in a cell fate shift towards a more mature skeletal cell phenotype, we asked whether, conversely, *Hoxa10* overexpression promotes stemness. We generated a lentiviral vector containing the protein-coding sequence of *Hoxa10* and that of *GFP* to mark infected cells (*LV-Hoxa10/GFP*), and a separate control vector containing only the *GFP* coding sequence (*LV-GFP*; **Fig. 4A**). The stable overexpression of *Hoxa10* was confirmed by qRT-PCR after infecting isolated periosteal stem and progenitor cells with *LV-Hoxa10/GFP* or *LV-GFP* (**Fig. 4B**). Compared to control PSPCs, which exhibited a large and broad shape morphology (**Fig. 4D**), *Hoxa10*-overexpressing PSPCs instead adopted a small, spindle shape morphology that is characteristic of typical mesenchymal stem cells ((Yang, Ogando et al. 2018); **Fig. 4D**). Moreover, seven days after infection, *Hoxa10* overexpressing periosteal cell cultures also had a significantly greater proportion of cells that expressed the stem cell markers PDGFRα, SCA1, and CD51 as assayed by flow cytometry (**Fig. 4C**). This is in accordance with the effect of *Hoxa10* on the hematopoietic system, where overexpression also increases the number of early hematopoietic progenitors

(Magnusson, Brun et al. 2007). These data indicate that *Hoxa10* overexpression promotes a stem cell state and thus we next decided to probe how *Hoxa10* may regulate the capacity of tibial stem and progenitors to differentiate.

Hoxa10-overexpressing periosteal stem and progenitor cells display deficient osteodifferentiation

Next, we investigated the effect of *Hoxa10* overexpression on the regulation of PSPC differentiation. Enforced expression of *Hox* genes blocks differentiation in numerous tissues and model organisms including *Hoxb4* and *Hoxa9* in lymphomyeloid differentiation (Owens and Hawley 2002, Schiedlmeier, Klump et al. 2003), *Hoxa5* during erythropoiesis (Crooks, Fuller et al. 1999, Fuller, McAdara et al. 1999), and *Hoxa2* during murine bone and cartilage development (Kanzler, Kuschert et al. 1998, Creuzet, Couly et al. 2002). The overexpression of *Hoxa10* inhibits commitment of early hematopoietic progenitors to the lymphomyeloid and erythroid lineages (Thorsteinsdottir, Sauvageau et al. 1997, Buske, Feuring-Buske et al. 2001, Taghon, Stolz et al. 2002, Magnusson, Brun et al. 2007) and blocks cardiac differentiation in cardiovascular progenitors (Behrens, Iacovino et al. 2013). This prompted us to ask whether *Hoxa10* plays a similar role in skeletal stem and progenitor cells of the tibia. To do so, we challenged *Hoxa10*-overexpressing cells to differentiate into the osteo-lineage (**Fig. 5A**). PSPCs that were infected with *LV-Hoxa10/GFP* and exposed to osteoinduction media for 14 days showed a more than 33% increase in the proportion of periosteal progenitors compared to those infected with the control virus, as measured by flow cytometry (**Fig. 5B**). *Hoxa10*-overexpressing cells also displayed lower expression of a suite of osteogenic genes (*Osterix*, *Osteocalcin*, and *Runx2)* after osteoinduction relative to control cells (**Fig. 5C**). Our findings suggest that *Hoxa10* overexpression either maintains cells in the stem cell-like state, while *LV-GFP* control cells begin to spontaneously differentiate or dysregulate – or *Hoxa10*-overexpressing cells are reprogrammed into a more stem cell-like state or a combination of both. We next investigated this proposition by probing the reprogramming abilities of *Hox* gene expression.

Hoxa10 overexpression mediates reprogramming of PP1 cells into PSCs

Several Hox family members (including their Drosophila orthologues) function as pioneer factors, demonstrating a strong preference to bind inaccessible chromatin and, by doing so, increase accessibility (Beh, El-Sharnouby et al. 2016, Bulajić 2019). Cellular reprogramming is associated with an opening of chromatin (Gaspar-Maia, Alajem et al. 2011, Ugarte, Sousae et al. 2015) and we previously showed that *Hox*-positive periosteal cells have more open chromatin and are more stem-like than periosteal cells derived from *Hox*-negative tissue (Bradaschia-Correa, Leclerc et al. 2019). This, along with the increase in stem cell frequency described above, led us to postulate whether *Hox* expression can drive skeletal progenitors to a more primitive state.

To investigate this, we sorted each periosteal stem and progenitor population (PSC, PP1, and PP2), and separately transduced them with either *LV-Hoxa10/GFP* or *LV-GFP*, and reassessed the lineage hierarchy to see if some cells could convert to a more primitive state (**Fig. 6A**). After 7 days of incubation, FACS analysis revealed that the sorted PSC population largely shifted toward the PP1 cell state, suggesting the PSCs rapidly differentiate to this more committed state in these culture conditions. However, no difference in cell populations within the PSPC lineage hierarchy was observed between PSCs transduced with *LV-Hoxa10/GFP* or *LV-GFP* (**Fig. 6C**). Strikingly, in sorted PP1 cells that were *LV-Hoxa10/GFP*-infected, FACS analysis revealed an increase in the more uncommitted stem cell compartment at the expense of the PP1 population after 7 days (16% converted cells); this proportional increase was limited in the *LV-GFP*-infected PP1 cells (5% converted cells)(**Fig. 6B, D, and Supplementary Fig. 3A**). This limited amount of stem cells in the control-infected PP1 cells may reflect a basal level of stochastic sampling of neighboring cellular states, as has been described in many other purified cell populations (Gupta, Fillmore et al. 2011, Wang, Quan et al. 2014). In contrast, PP2 cells showed no difference in the relative abundance of the different cell populations when overexpressing *Hoxa10* (**Fig. 6E**). Multiple independent iterations of this experiment confirmed these results, in which *Hoxa10*-overexpressing PP1 cells led to a greater than two-fold increase in the proportion of uncommitted periosteal stem cells among cells in the PSPC compartment (**Fig. 6F; Table 1**) and around a three-fold increase in the frequency of PSCs among total *Hoxa10*-overexpressing cells (**Fig. 6G**).

To examine the possibility that *Hoxa10* overexpression merely triggers proliferation of the more uncommitted periosteal cells, we employed CellTrace™ to assess the cycling rate of each stem and progenitor compartment infected with *LV-Hoxa10/GFP* or *LV-GFP*. In these experiments, *Hoxa10* overexpression did not increase the proliferative rate of PSPCs (**Fig. 6H, Supplementary Fig. 3B**). This contrasted with the *Hox* knockout and *si*RNA knockdown experiments in which *Hox* expression had a significant influence on proliferative capacity (**Fig. 3**). One explanation may be that there is a maximum proliferation rate that PSPC populations can reach. Consistent with this, studies have shown that PSPCs are already highly proliferative, displaying the highest proliferative capacity when compared to other mesenchymal progenitor populations derived from different tissues (Sakaguchi, Sekiya et al. 2005, Yoshimura, Muneta et al. 2007, van Gastel, Torrekens et al. 2012, Duchamp de Lageneste, Julien et al. 2018). We further confirmed the insignificance of proliferation for PSC conversion by inhibiting proliferation in PP1 *Hoxa10*-overexpressing cells via mitomycin C treatment. After confirming effective inhibition of proliferation (**Supplementary Fig. 3C**), we again examined the lineage hierarchy and observed a cell fate switch from the progenitor to the more primitive stem cell (**Fig. 6I**). Interestingly, the magnitude of the conversion was much larger than in the case of PP1 cells with unaltered proliferative capacity. Mitomycin C is known to arrest cells in the G1 phase of the cell cycle (Kang, Chung et al. 2001) and multiple studies have connected cell fate decisions to a prolonged G1 (Sela, Molotski et al. 2012, Tapias, Zhou et al. 2014). It may be that PP1 cells in cell cycle arrest create a more permissive window for cell reprogramming factors to change their cell state. Overall, these data highly suggest that the expansion of stem cells among total cells and within the PSPC compartment is due to progenitors reprogramming to a less committed state.

To further assess whether the more committed PP1 cells have genuinely been reprogrammed to a periosteal stem cell fate, we utilized published single-cell gene expression data (Debnath, Yallowitz et al. 2018) to identify new transcriptional markers of periosteal stem cells. We sorted cells *in silico* using the previously defined PSPC cell surface markers and uncovered several new factors that were additionally enriched in periosteal stem cells versus PP1 and PP2 cells (*Omd*, *Car3*, *Ucma*, and *Frzb* (**Supplementary Fig. 4A**). Gene expression analysis of PP1 cells transduced with *LV-Hoxa10/GFP* by qRT-PCR

revealed a higher expression of these newly identified periosteal stem cell marker genes relative to those infected with *LV-GFP* (**Supplementary Fig. 4B**), indicating a more comprehensive shift towards the distinct stem cell transcriptome as cells are reprogrammed. Stem cells are defined by their capacity to self-renew and differentiate. PSCs are at the top of the periosteal skeletal stem and progenitor lineage hierarchy and thus possess a greater ability to self-renew during serial transplantation assays relative to PP1 and PP2 cells (Debnath, Yallowitz et al. 2018). To investigate whether PP1 *Hoxa10*-overexpressing cells are functionally reprogrammed to a stem cell state, we interrogated their competence to self-renew using a serial transplantation assay in which PP1 cells are first infected with either *LV-Hoxa10/GFP* or *LV-GFP*, and 300 to 750 GFP^+ cells are isolated and transplanted (along with 100,000 bone marrow support cells) underneath the renal capsule for two weeks – an environment that promotes differentiation of mesenchymal stem cells (Debnath, Yallowitz et al. 2018, Ambrosi, Marecic et al. 2021). GFP^+ cells were then re-sorted and re-transplanted for a further two weeks and the persistence of GFP^+ PSCs (reprogrammed from PP1 cells) was determined following each transplantation (**Fig. 6J**). Indeed, flow cytometry of post-transplantation cells revealed that GFP+ PSCs derived from control *LV-GFP*-infected PP1 cells were largely lost over time when compared to the pre-transplantation frequency. In contrast, PSCs derived from *LV-Hoxa10/GFP*-infected PP1 cells were maintained to a larger degree after multiple rounds of transplantation, indicating a greater self-renewal capacity (**Fig. 6K, L**). With the capacity of *Hoxa10* to shift periosteal progenitors of the tibia towards less committed state that possesses greater self-renewal capacity, these results highlight a master role for *Hox* genes in the regulation of skeletal stem cells.

The regional specificity of Hox function is maintained in the adult skeleton

Previous studies, including findings from our own lab, showed that *Hox* gene expression is maintained in adult skeletal elements other than the tibia and that the expression patterns roughly mirror the regionally restricted expression during embryogenesis (**Fig. 7I**) (Ackema and Charite 2008, Leucht, Kim et al. 2008, Rux, Song et al. 2016, Rux and Wellik 2017, Bradaschia-Correa, Leclerc et al. 2019, Song, Pineault et al. 2020). Thus, as in development, the adult “Hox code” may endow stem cells from different anatomical locations

with the specific functional properties needed to successfully regenerate the tissue in which they reside. While periosteal cells derived from distinct skeletal regions exhibit functional differences that are correlated with differential *Hox* expression (Leucht, Kim et al. 2008, Bradaschia-Correa, Leclerc et al. 2019), the regional specificity of *Hox* function in the adult has not been definitively established. To investigate this, we asked whether *Hoxa10* functions in a universal manner in stem and progenitor cells from any part of the skeleton or whether its stem cell maintenance function is limited to the tibia, with, perhaps, other *Hox* genes filling that role in other regions. First, we isolated periosteal cells from various skeletal elements, including the pelvis, the thoracic vertebrae 5 through 8 of the spine, the radius/ulna, and anterior ribs 1 through 4 (**Fig. 7A**), and subjected them to gene expression analysis using the Nanostring nCounter® technology to uncover the *Hox* expression profiles of all 39 *Hox* genes among these four tissues. We found that, as in the tibia, *Hoxa10* is the most highly expressed family member in periosteal cells of the pelvis and radius/ulna (**Fig. 7A, E**; **Supplemantary Fig. 6**). In the adult spine$^{T5\text{-}8}$ periosteum, *Hoxb8* is the highest expressed (**Fig. 7C; Supplementary Fig. 6**), reflecting the developmental expression profile as this section of the vertebral column is configured by the Hox8 group (Favier and Dolle 1997, van den Akker, Reijnen et al. 1999). Finally, *Hoxa5* is the most highly expressed *Hox* gene in the anterior ribs$^{1\text{-}4}$ (**Fig. 7G**).

Periosteal progenitors were then isolated from each anatomical region and infected with either control, *Hoxa10*, or the Hox gene shown to be most highly expressed in that region. In the pelvis, spine$^{T5\text{-}8}$, and anterior ribs$^{1\text{-}}$4, PP1 cells were only reprogrammed to a PSC state when transduced with their correct regional-specific Hox gene (**Fig. 7; Supplementary Fig. 6; Table 2**). PP1 cells overexpressing a Hox gene from another region, for example, *Hoxa10* expression in periosteal cells from the spine or rib, did not enhance reprogramming relative to the control virus. Interestingly, in the radius/ulna towards a stem cell fate despite being the most expressed Hox gene in the periosteum of this region. *Hoxa11*, however, is also very highly expressed in this skeletal element and *Hoxa11* lentiviral overexpression in this region induced reprogramming of radius/ulna PP1 cells. It is noteworthy that in whole-body knockouts of *Hoxa10*, only minor skeletal defects in the radius and ulna are observed when compared to defects that arise in *Hoxa11* mutants (Small and Potter 1993, Davis, Witte et al. 1995, Favier, Rijli et al. 1996, Boulet and Capecchi 2002, Wellik and Capecchi

2003), suggesting that the function of periosteal cells in this region may be more influenced by *Hoxa11*.

As embryonic development progresses anterior-to-posterior (and proximal-to-distal in the limbs), each Hox gene cluster successively becomes more accessible and expressed, generating a nested pattern where more posterior tissues express a wider set of Hox genes than anterior ones (Tarchini and Duboule 2006, Papageorgiou 2012). This prompts the hypothesis that more posterior tissues may respond to anterior *Hox* gene expression. To test this, we infected tibial PP1 cells with *Hoxa5*-overexpressing or control lentivirus. *Hoxa5* overexpression in these posterior progenitor cells did not induce reprogramming (**Supplementary Fig. 7A**). Along with Hoxa10, Hoxa11 is also highly expressed in tibia periosteal cells and, when overexpressed, triggered tibia periosteal progenitor cells to revert to a more primitive state (**Supplementary Fig. 7B**). Altogether, these results reveal a model in which *Hox* genes function to maintain periosteal stemness and as reprogramming modulators in a regionally restrictive manner – and suggests that there is a limited set of 'flanking' Hox genes to which periosteal progenitors can respond. Importantly, this may have wider implications on the engraftment potential of future cell transplant therapies where tissue is often taken from one part of the body and transplanted into another.

Discussion

Skeletal homeostasis and regeneration rely heavily on stem cells to replenish the tissue lost due to injury or wear and tear. To preserve this capacity, stem cell number has to be constantly maintained by cell division, one of the hallmarks of stemness. There is a relatively poor understanding of the molecular mechanisms that govern skeletal stem and progenitor cell maintenance and lineage progression during bone healing, and this presents one of the major hurdles to advancing cell-based therapies for treatment of bone fractures. This investigation adds to the growing appreciation that *Hox* genes have important maintenance functions in the adult skeleton. The experiments herein support a model in which high expression of *Hox* genes in the most uncommitted periosteal cell compartments confers greater proliferative ability, self-renewal capacity, and inhibits lineage progression towards

more committed cell fates. They also demonstrate that this role of Hox can be exploited to shift periosteal progenitors with limited self renewal capacity (Debnath, Yallowitz et al. 2018) to a more primitive state, thus increasing their functional potential.

Previous reports have identified *Hoxa11* as the primary *Hox* gene that patterns the embryonic tibia and is a marker of the adult tibia (Wellik and Capecchi 2003, Rux, Song et al. 2016) Our work revealed that *Hoxa10*, not *Hoxa11*, is the highest expressed Hox gene in the tibial periosteum (**Supplementary Fig. 1**). Although the Hox11 group is regionally restricted to both the radius/ulna and the tibia/fibula in the adult (Rux, Song et al. 2016), only the radius and ulna fail to develop in Hoxa11/Hoxd11 double mutants. The tibia and fibula are only lightly affected (Davis, Witte et al. 1995, Wellik and Capecchi 2003), suggesting that these genes play a more substantial role in the forelimbs. As we identified *Hoxa10* as the most expressed Hox gene in the adult tibia periosteum, we hypothesized that this paralog may have a functional role in this skeletal element. To date, only whole embryonic (non-inducible) *Hox10* group knockouts have been studied. Both *Hoxa10*$^{-/-}$ and *Hoxd10*$^{-/-}$ mice display skeletal patterning alterations in the developing hindlimbs, with changes in these structures appearing with greater penetrance in *Hoxa10*$^{-/-}$ mice (Wahba, Hostikka et al. 2001).

While recent studies demonstrate that *Hoxa11* marks a primitive mesenchymal stem cell (MSC) in the periosteum and that *Hoxa11*-lineage marked cells are long-term contributors to MSCs throughout life (Rux, Song et al. 2016, Pineault, Song et al. 2019, Song, Pineault et al. 2020), we show for this first time that *Hox* genes play a stem cell maintenance function in the skeletal system. During differentiation of osteoblastic cell lines, HOXA10 drives the early expression of osteogenic genes through chromatin remodeling, and the *in vivo* conditional deletion of *Hoxa11* and *Hoxd11* in the *Hoxa11* domain leads to osteogenic differentiation defects (Hassan, Tare et al. 2007, Song, Pineault et al. 2020) suggesting a role for some Hox genes at later stages of cell fate commitment. Notably, using a *Hoxa11* knock-in reporter that simultaneously deletes *Hoxa11* coding sequence, *Song et al.* found that skeletal stem cells expressing the reporter are still present 10 months after the conditional deletion of *Hoxa11* and *Hoxd11 alleles* in 8-week-old forelimbs (Song, Pineault et al. 2020), presumably precluding a stem cell maintenance role for *Hox* genes. These

studies focus on the *Hox11* paralogous group, however, and disregard the potential functional redundancy of other *Hox* groups expressed at high levels in the skeletal cells under study – as we observe in the tibia periosteum (**Fig. 2A, Supplementary Fig. 1**).

Recent loss-of-function studies in various tissues have demonstrated a stem cell maintenance role for *Hox* genes although phenotypes have usually been mild (Magli, Largman et al. 1997, Owens and Hawley 2002, Bjornsson, Larsson et al. 2003, Brun, Bjornsson et al. 2004, Iyyanar and Nazarali 2017). Additionally, *Rux et al.* have recently shown that skeletal stem cells harvested from mice in which both alleles of *Hoxd11* and one allele of *Hoxa11* are knocked out display tri-lineage differentiation dysfunction but do not lose their stemness marker profile or self-renewal capacity (Rux, Song et al. 2016). These studies typically rely on reducing the expression of one *Hox* paralogous group (or use single *Hox* knockout mouse models), however, and disregard the potential complementation by other highly expressed *Hox* genes in the cells compartment under study – as observed in the tibia periosteum (**Supplementary Fig. 1A, B**). The examination of compound mutants or deficiencies within a *Hox* cluster or paralogous group may therefore yield more severe phenotypes that can elucidate the role of *Hox* in adult skeletal cells. Here, our work shows that the expression of multiple posterior *Hox* paralogous groups must be decreased to detect a defect in number and function of tibial PSPCs; a reduction of part of the *Hox10* and *11* groups was not sufficient to reveal this phenotype (data not shown). This redundancy may represent an evolutionary mechanism to maintain stem cells.

Overall, the integration of these findings suggests a model in which, initially, the overlapping expression of several similar *Hox* paralogs collectively maintains skeletal stem cell function, after which individual *Hox* genes impart specific functions in the committed progenitor populations that direct their differentiation. This regulatory pattern would not be unprecedented in the context of *Hox*. In the developing Drosophila heart, forced expression of *Abd-B* (the orthologue of the posterior *Hox9-13* genes in mammals) inhibits cardiac myogenesis of mesodermal cells, underscoring its capacity to inhibit cell fate commitment in this tissue. Later during heart development, however, *Abd-B* expression is detectable in the more committed cells of the heart tube, precluding an inhibitory role at this later stage

(Lovato, Nguyen et al. 2002).

In bone and other tissues, overlapping *Hox* genes show preferential activities that are consistent with a model of both simultaneous redundancy and specificity of *Hox* function (Shen, Montgomery et al. 1997, Shen, Rozenfeld et al. 1997, Pineault, Helgason et al. 2002, Akbas and Taylor 2004, Hedlund, Karsten et al. 2004). Thus, the observed co-expression of multiple *Hox* genes in periosteal cells highlight a probable complex combinatorial function in their regulation of primitive skeletal tissues. Further investigation of the transcriptional targets of HOX factors in distinct skeletal stem and progenitor cell populations may provide insight into their precise spatiotemporal and cell-type-specific roles.

The inability of *Hoxa10* overexpression to reprogram more committed PP2 progenitors is noteworthy. Cells that have progressed along the lineage trajectory and become fate-restricted likely undergo chromatin remodeling events that may inhibit HOX transcription factors from accessing the genes that regulate stem cell activity – enabling them to instead regulate differentiation genes as proposed above – but these hypotheses remain to be verified. Our previous work showed that the calvarial periosteum exhibits a near absence of *Hox* expression, contains more fate-restricted cells, and more inaccessible chromatin (Bradaschia-Correa, Leclerc et al. 2019). When we ectopically induced *Hox* expression in this cell population, we did not observe an upregulation of stem cell markers or an increase in calvarial PSPC number, as with tibial PSPCs (**Fig. 4, Supplementary Fig. 5**). This is in accordance with the notion that chromatin remodeling in more committed cells may prevent reprogramming by *Hox*.

The continued regional specification of *Hox* gene expression in adult tissues has been demonstrated by several independent studies, largely by the characterization of cells in culture (Chang, Chi et al. 2002, Leucht, Kim et al. 2008, Bradaschia-Correa, Leclerc et al. 2020). Here we corroborate this finding in the periosteal cell compartments of various anatomical regions and, importantly, find that this adult Hox code is functionally relevant to skeletal stem cell regulation. Region-specific *Hox* function in reprogramming and stem cell maintenance has implications for devising stem cell therapies that target specific segments

of the skeleton, or potentially other tissues whose function is controlled by *Hox* expression profiles.

Relative to the bone marrow, the periosteum is a new, relatively understudied field of research. Periosteal progenitor cells play a central role in bone repair and, as such, represent a promising source of cells for tissue engineering approaches. PSPCs also exhibit a number of characteristics that are advantageous for such strategies, including their high proliferative rate necessary for efficient *in vitro* expansion (Sakaguchi, Sekiya et al. 2005, Yoshimura, Muneta et al. 2007, van Gastel, Torrekens et al. 2012), and a greater osteogenic capacity than many other mesenchymal stem cell populations both *in vitro* and when transplanted *in vivo* (Roberts, Geris et al. 2011, Roberts, van Gastel et al. 2015). Looking forward, advances in lineage reprogramming in many tissues have revealed a remarkable flexibility in cell identity (Morris 2016), and unraveling the mechanisms of this process in skeletal tissues can facilitate the development of cell fate engineering strategies. Further research examining how *Hox* overexpression increases stem cell potency along with the downstream genetic elements that mediate it – and investigating whether it does so without affecting lineage potential – can help achieve this therapeutic goal.

Materials & Methods

Animals

C57BL/6 mice, 8- to 16-week-old, were purchased from the Jackson Laboratory (Bar Harbor, ME) and bred in the barrier facility at the New York University School of Medicine. *Pdgfra*$^{CreERT/+}$ knock-in mice were obtained from by the Michael Wosczyna Laboratory at NYU Langone (Wosczyna, Konishi et al. 2019). *Osx*$^{CreERT2/+}$ mice were received from Dr. H. M. Kronenberg, Massachusetts General Hospital. *Col1a1*$^{CreERT/+}$ mice (B6.Cg-Tg(Col1a1-cre/ERT2)1Crm/J) were obtained from JAX (016241). All mice were bred in the barrier facility at the New York University School of Medicine. To induce recombination in transgenic cre-

ERT2 mice, tamoxifen (Sigma-Aldrich, St. Louis, MO, USA) was administered intraperitoneally either 2 mg/day according to the dosing protocol in **Figure 3A**. Mice were maintained on a 12-h light/dark cycle with food and water provided ad libitum.

Patients and Specimens.

All experiments involving human subjects were ap- proved by the New York University (NYU) School of Medicine Institutional Review Board. After informed consent was obtained, bone marrow specimens were obtained during surgery at the fracture site. One cubic centimeter of bone marrow was immediately transferred into a microcentrifuge tube and placed on ice.

Bulk RNA sequencing and Nanostring

FPKM values for each *Hox* gene was derived from tibial periosteal RNA sequencing data previously published by our group (Bradaschia-Correa, Leclerc et al. 2019) and $CD45^{-}$ $TER119^{-}CD31^{-}LEPR^{+}$ also published by our group (Josephson, Bradaschia-Correa et al. 2019). Nanostring™ read counts were determined using the nCounter platform and by generating a custom panel of target-specific oligonucleotide probes (CodeSet) of the 39 murine *Hox* genes (**Table 3**). Of the total 78 Hox isoforms produced by the four Hox clusters, only one isoform of Hoxc4 was not detectable by the custom CodeSet. Five housekeeping genes (*Actb*, *Gusb*, *Pgk1*, *Tbp*, *Tubb*) were used to normalize the read counts.

Periosteal Cell Isolation

Primary periosteal stem and progenitor cells were obtained from the tibia, pelvis, anterior ribs (1-4), thoracic vertebrae (5-8) of the spine, radius/ulna, or parietal/frontal calvaria. After careful dissection from 8 to 16-week-old wild type (C57BL/6) mice, bones with intact periosteum were submitted to 4 serial collagenase digestions in 0.2% collagenase type 2 (ThermoFisher Scientific: 17101015) in DMEM (Life Technologies: 11885092) at 37 °C for 20 minutes with gentle rocking. After each of the first three digestions, bones were subjected to light centrifugation (1000 rpm) for 5 min and then transferred to a fresh tube of collagenase. After the last digestion, bones were centrifuged at 1400 rpm for 5 min and the pelleted cells were resuspended in growth media (GM): low glucose DMEM (Life Technologies: 11885092), 10% Fetal Bovine Serum (Life Technologies: 10437-028), 1% Penicillin/Streptomycin (Life Technologies: 15140122). Selective enrichment of periosteal stem/progenitor cells was confirmed using FACS analysis (**Supplementary Fig. 1C**).

Flow Cytometry

Cells were trypsinized, resuspended in HBSS (Life Technologies: 14170161), supplemented with 2% Fetal Bovine Serum (Life Technologies: 10437-028), 1% Penicillin/Streptomycin (Life Technologies: 15140122), and 1% HEPES (Life Technologies: 15630080) (complete HBSS), and stained with 1:300 diluted CD45-PE (Miltenyi Biotec: 130-117-498), TER119-PE (Miltenyi Biotec: 130-117-512, TIE2-PE (ThermoFisher Scientific: 12-5987-82), 6C3-PE (ThermoFisher Scientific: 12-5891-82), CD90-PE (Invitrogen: MA5-17749), and 1:200 diluted CD51-BV421 (BD Biosciences: 740062), CD105-PE-Cy7 (ThermoFisher Scientific: 25-1051-82) , CD200-BV711 (BD Biosciences: 745548) for 30 minutes on ice in the dark. Cells were then washed with 1mL of the complete HBSS solution, centrifuged at 1500 rpm for 5 minutes and finally resuspended with complete HBSS for flow cytometry. Cells were sorted on a Sony Biotechnology SY3200^{TM} cell sorter into a 50%/50% solution of complete HBSS and Fetal Bovine Serum or analyzed on a Bio-Rad ZE5 Analyzer. Sorting was validated to result in >95% purity of the intended population in postsort fractions. Beads

(eBioscience 01-1111-41) were used to set initial compensation. Fluorescence minus one (FMO) controls were used for additional compensation and to assess background levels for each stain. We excluded doublets and gates were drawn as determined by internal FMO controls to separate positive and negative populations for each cell surface marker. Mesenchymal cell populations negative for CD45, CD31 and Ter119 cell surface markers were analyzed according to the approach described in Supplementary figure 2d.

in vitro Differentiation

5 x 10^4 PSPCs or sorted PP1 cells were seeded onto individual wells of 24-well plates (wells were first coated with a 1:100 dilution of fibronectin [Sigma: F0895] in PBS for 60 mins) in GM and allowed to attach overnight. The next day, cells were stimulated with osteogenic media (OM) [DMEM, 10% FBS, 100 µg/mL ascorbic acid, 10 mM β-glycerophosphate, and 1% penicillin/streptomycin]. Media was replenished every 2-3 days. For adipogenic differentiation, the cells were induced the next day using the MSC Adipogenic BulletKit (Lonza, Allendale, NJ) induction media.

RNA Interference

Primary PSPCs were transfected with Qiagen's commercially available GeneSolution siRNAs targeting *Hoxa10* (CAGGGCCCAGCCAAACTCCAA; SI00201859), *Hoxd10* (CCGAACAGATCTTGTCGAATA; SI00206542), *Hoxc10* (CAGGGCCCAGCCAAACTCCAA; SI00201859), *Hoxa11* (CACCACTGATCTGCACCCAAA; SI01068788), and *Hoxd11* (CCCGTCGGACTTCGCCAGCAA; SI01069558). AllStars Negative Control siRNA (Qiagen, 1027281) was used as a non-targeting control. Each component siRNA of *HoxMix* was delivered at 5µM, yielding a total *HoxMix* concentration of 25µM; non-targeting control siRNA was delivered at 25µM. HiPerfect Transfection Reagent (Qiagen) was used as a transfection

reagent as per manufacturer's instructions. Transfection was carried out at the moment of seeding onto multiwell plates before the cells fully attached to the plates (fast-forward transfection). The seeded cells were treated with siRNAs every 3 to 4 days and samples were assayed by qRT-PCR or flow cytometry after 2 to 14 days of knockdown.

Proliferation Assay

5 x 10^4 PSPCs were seeded onto wells of 24-well plates in GM and simultaneously administered either *HoxMix* or nontargeting siRNAs. After 24 hours, the cells were incubated with 10μM EdU at 37°C for 15 hours, washed with PBS, and then trypsinized. The Click-iT™ Plus EdU Alexa Fluor™ 488 Flow Cytometry Kit (ThermoFisher Scientific, C10632) was utilized to fix, permeabilize, and label EdU-incorporated cells with a Click-iT™ reaction as per the manufacturer's instructions before subjecting the cells to flow cytometry analysis thereafter.

Cell-Cycle Analysis

CellTrace™ Far Red Cell Proliferation Kit (ThermoFisher Scientific: C34564) was used per manufacturer's instructions. In the RNA interference expreiments, PSPCs isolated from C57BL/6 wild-type mice were first expanded in vitro, and 5 x 10^4 cells were then seeded onto individual wells of a 24-well plate with *HoxMix* or nontargeting siRNA. 24 hours later, the cells from each well were trypsinized, incubated with CellTrace™ for 1 hour at 37°C on day 0, then replated and cultured for 6 days. On day 6, cells were trypsinized and stained for PDGFRα (Invitrogen: 25-1401-82). A separate batch of cells was also trypsinized and incubated with CellTrace™ for 1 hour at 37°C on day 6 to serve as a positive control.
For the overexpression experiments, PSCs, PP1, and PP2 cells were sorted from *in vitro*-expanded PSPCs. 3 x 10^4 cells were incubated with either *LV-GFP* or *LV-Hoxa10/GFP* in individual wells of a 24-well plate. After 24 hours, the procedure was then continued as described above. Cells in this case were stained with the *Debnath et al.*-defined lineage cell surface markers previously described.

Cells were then analyzed on a BD Biosciences LSRII UV cell analyzer for dye dilution and surface marker profile.

RNA Isolation and Quantitative Real-Time PCR

RNA was either isolated from cells immediately following periosteal isolation and FACS to observe *in vivo* gene expression or from cells expanded *in vitro*. The RNeasy Plus Kit (Qiagen: 74134) was used to isolate RNA and remove genomic DNA, and RNA was then reverse-transcribed with the iScript cDNA Synthesis Kit (Bio-Rad: 170-8891). Quantitative real-time PCR was carried out using the Applied Biosystems QuantStudio3 system and RT^2 SYBR Green ROX PCR Master Mix (Qiagen: 330523). Specific primers were designed using Harvard PrimerBank (http://pga.mgh.harvard.edu/primerbank/) (**Table 4**). Results are presented as $2^{-\Delta\Delta Ct}$ values normalized to the expression of *18s*. Means and SEMs were calculated in GraphPad Prism 7 software.

Viral Generation and Transduction

Lentiviral DNA containing either a *Hoxa10* CDS expression construct or a control construct lacking *Hoxa10* CDS was generated at Genewiz (New Jersey) using the Tet-ON system. In addition to the Hoxa10 sequence, the lentiviral vector used (*ptetO*) also include EGFP, Luciferase, and Puromycin cloned downstream of the active CMV promoter. 2A peptide sequences are also included between each element (*ptetO-Hoxa10-T2A-EGFP-P2A-Luciferase-T2A-Puromycin*; *LV-Hoxa10/GFP*) (*ptetO-EGFP-P2A-Luciferase-T2A-Puromycin*; *LV-GFP*) in order to produce multi-cistronic, equimolar expression of all four genes. EGFP was used to track the cells that have been infected in culture. Identical methods were used to generate lentiviral sequences containing *Hoxa11*, *Hoxb8*, and *Hoxa5*. *pLenti-rtTA3* (Addgene: 26429), *pRSV-Rev* (Addgene: 12259), *pMD2.G* (Addgene: 12259), and *pMDLg/pRRE* (Addgene: 12251) plasmids were purchased and lentivirus was generated in the Lenti-X™ 293T Cell Line (TakaraBio: 632180), purified with a Lenti-X™

Maxi Purification Kit (TakaraBio: 631234), and titered with a Lenti-X qRT-PCR Titration Kit (TakaraBio: 631235).

3 x 10^4 sorted PSCs, PP1, PP2, or *in vitro*-expanded PSPCs were seeded onto individual wells of 24-well plates (wells were first coated with a 1:100 dilution of fibronectin [Sigma: F0895] in PBS for 60 mins) using GM made with 10% heat-inactivated Fetal Bovine Serum and 1% Penicillin/Streptomycin. The cells were immediately transduced with *pLenti-rtTA* and either *LV-GFP*, *LV-Hoxa10/GFP*, *LV-Hoxa11/GFP*, *LV-Hoxb8/GFP*, or *LV-Hoxa5/GFP* at an M.O.I. of 75. The transduction efficiency was aided by the addition of 2.5 µg/mL Polybrene (Sigma) and the cells were treated 10 µg/mL Doxycycline to activate expression downstream of the tetO promoter sequences. GM with 10 µg/mL Doxycycline was used to replace the media every 2-3 days.

Identification of PSC Markers from Dataset

The periosteal scRNA-seq dataset is from a publicly available adult mouse femoral periosteum study (Debnath, Yallowitz et al. 2018). We obtained the raw count matrix from the GEO accession ID GSE106236 and annotated cells based on high expression levels of the genes associated with the cell surface markers used for flow cytometry [6C3 (*Enpep*), CD90 (*Thy1*), CD51 (*Itgav*), CD105 (*Eng*), and CD200 (*Cd200*)]. The PSC, PP1, and PP2 cells in the count matrix were then sorted *in silico* according to the *Debnath et al.*-derived gating strategy presented in the results, and genes with a high fold change between PSCs and PP1/PP2 cells were used to identify potential PSC markers.

Renal Capsule Transplants

A model of mesenchymal stem cell differentiation was used to compare the regenerative potential of PSPCs. 12- to 15-week-old, syngeneic C57BL/6 mice were used as hosts for the renal capsule transplantation assay. An incision was made on the dorsal skin surface, followed by an incision through the peritoneum, the kidneys were identified and then

exteriorized. An incision in the renal capsule was made using a 27-gauge needle. Two microliters of tibial bone marrow (containing ~100,000 cells) from 12-week-old C57BL/6 mice were used to resuspend 750 transduced (GFP^+) PP1 cells. The mixture was then left exposed to open air for one to two minutes to allow for a limited amount of coagulation and subsequently grafted beneath the capsule. The kidney was placed back into its anatomic location and the peritoneum was closed with a Vicryl suture, followed by skin closure with a 6-0 Vicryl suture. Mice had ad lib access to food and water (with dissolved .4 mg/mL Doxycycline and 5% sucrose) and received subcutaneous buprenorphine for analgesia. Mice were euthanized 14 days post-surgery, the renal grafts were harvested, digested in 0.2% collagenase type 2 (ThermoFisher Scientific) in DMEM at 37°C for 1 hour, stained with antibodies, and subjected to FACS. The GFP^+ cells were collected and reused for the subsequent renal grafts.

References

Ackema, K. B. and J. Charite (2008). "Mesenchymal stem cells from different organs are characterized by distinct topographic Hox codes." Stem Cells Dev **17**(5): 979-991.

Akbas, G. E. and H. S. Taylor (2004). "HOXC and HOXD gene expression in human endometrium: lack of redundancy with HOXA paralogs." Biol Reprod **70**(1): 39-45.

Ambrosi, T. H., M. T. Longaker and C. K. F. Chan (2019). "A Revised Perspective of Skeletal Stem Cell Biology." Front Cell Dev Biol **7**: 189.

Ambrosi, T. H., O. Marecic, A. McArdle, R. Sinha, G. S. Gulati, X. Tong, Y. Wang, H. M. Steininger, M. Y. Hoover, L. S. Koepke, M. P. Murphy, J. Sokol, E. Y. Seo, R. Tevlin, M. Lopez, R. E. Brewer, S. Mascharak, L. Lu, O. Ajanaku, S. D. Conley, J. Seita, M. Morri, N. F. Neff, D. Sahoo, F. Yang, I. L. Weissman, M. T. Longaker and C. K. F. Chan (2021). "Aged skeletal stem cells generate an inflammatory degenerative niche." Nature **597**(7875): 256-262.

Bardin, A. J., C. N. Perdigoto, T. D. Southall, A. H. Brand and F. Schweisguth (2010). "Transcriptional control of stem cell maintenance in the Drosophila intestine." Development **137**(5): 705-714.

Beh, C. Y., S. El-Sharnouby, A. Chatzipli, S. Russell, S. W. Choo and R. White (2016). "Roles of cofactors and chromatin accessibility in Hox protein target specificity." Epigenetics Chromatin **9**: 1.

Behrens, A. N., M. Iacovino, J. L. Lohr, Y. Ren, C. Zierold, R. P. Harvey, M. Kyba, D. J. Garry and C. M. Martin (2013). "Nkx2-5 mediates differential cardiac differentiation through interaction with Hoxa10." Stem Cells Dev **22**(15): 2211-2220.

Bjornsson, J. M., N. Larsson, A. C. Brun, M. Magnusson, E. Andersson, P. Lundstrom, J. Larsson, E. Repetowska, M. Ehinger, R. K. Humphries and S. Karlsson (2003). "Reduced proliferative capacity of hematopoietic stem cells deficient in Hoxb3 and Hoxb4." Mol Cell Biol **23**(11): 3872-3883.
Boulet, A. M. and M. R. Capecchi (2002). "Duplication of the Hoxd11 gene causes alterations in the axial and appendicular skeleton of the mouse." Developmental Biology **249**(1): 96-107.
Bradaschia-Correa, V., K. Leclerc, A. M. Josephson, S. Lee, L. Palma, H. P. Litwa, S. S. Neibart, J. C. Huo and P. Leucht (2019). "Hox gene expression determines cell fate of adult periosteal stem/progenitor cells." Sci Rep **9**(1): 5043.
Bradaschia-Correa, V., K. Leclerc, A. M. Josephson, S. Lee, L. Palma, H. P. Litwa, S. S. Neibart, J. C. Huo and P. Leucht (2020). "Author Correction: Hox gene expression determines cell fate of adult periosteal stem/progenitor cells." Sci Rep **10**(1): 3220.
Brun, A. C., J. M. Bjornsson, M. Magnusson, N. Larsson, P. Leveen, M. Ehinger, E. Nilsson and S. Karlsson (2004). "Hoxb4-deficient mice undergo normal hematopoietic development but exhibit a mild proliferation defect in hematopoietic stem cells." Blood **103**(11): 4126-4133.
Bulajić, M. S., D.; Dasen, J.S.; Wichterle, H.; Mahony, S.; Mazzoni, E.O. (2019). "Hox binding specificity is directed by DNA sequence preferences and differential abilities to engage inaccessible chromatin." bioRxiv.
Buske, C., M. Feuring-Buske, J. Antonchuk, P. Rosten, D. E. Hogge, C. J. Eaves and R. K. Humphries (2001). "Overexpression of HOXA10 perturbs human lymphomyelopoiesis in vitro and in vivo." Blood **97**(8): 2286-2292.
Carpenter, E. M., J. M. Goddard, O. Chisaka, N. R. Manley and M. R. Capecchi (1993). "Loss of Hox-A1 (Hox-1.6) function results in the reorganization of the murine hindbrain." Development **118**(4): 1063-1075.
Chan, C. K. F., E. Y. Seo, J. Y. Chen, D. Lo, A. McArdle, R. Sinha, R. Tevlin, J. Seita, J. Vincent-Tompkins, T. Wearda, W.-J. Lu, K. Senarath-Yapa, M. T. Chung, O. Marecic, M. Tran, K. S. Yan, R. Upton, G. G. Walmsley, A. S. Lee, D. Sahoo, C. J. Kuo, I. L. Weissman and M. T. Longaker (2015). "Identification and specification of the mouse skeletal stem cell." Cell **160**(1-2): 285-298.
Chang, H. Y., J. T. Chi, S. Dudoit, C. Bondre, M. van de Rijn, D. Botstein and P. O. Brown (2002). "Diversity, topographic differentiation, and positional memory in human fibroblasts." Proc Natl Acad Sci U S A **99**(20): 12877-12882.
Cheng, A., C. E. Vantucci, L. Krishnan, M. A. Ruehle, T. Kotanchek, L. B. Wood, K. Roy and R. E. Guldberg (2021). "Early systemic immune biomarkers predict bone regeneration after trauma." Proc Natl Acad Sci U S A **118**(8).
Christen, B., C. W. Beck, A. Lombardo and J. M. Slack (2003). "Regeneration-specific expression pattern of three posterior Hox genes." Dev Dyn **226**(2): 349-355.
Colnot, C., X. Zhang and M. L. Knothe Tate (2012). "Current insights on the regenerative potential of the periosteum: molecular, cellular, and endogenous engineering approaches." J Orthop Res **30**(12): 1869-1878.
Costa, L. A., N. Eiro, M. Fraile, L. O. Gonzalez, J. Saa, P. Garcia-Portabella, B. Vega, J. Schneider and F. J. Vizoso (2021). "Functional heterogeneity of mesenchymal stem cells from natural niches to culture conditions: implications for further clinical uses." Cellular and Molecular Life Sciences **78**(2): 447-467.

Creuzet, S., G. Couly, C. Vincent and N. M. Le Douarin (2002). "Negative effect of Hox gene expression on the development of the neural crest-derived facial skeleton." Development **129**(18): 4301-4313.
Crooks, G. M., J. Fuller, D. Petersen, P. Izadi, P. Malik, P. K. Pattengale, D. B. Kohn and J. C. Gasson (1999). "Constitutive HOXA5 expression inhibits erythropoiesis and increases myelopoiesis from human hematopoietic progenitors." Blood **94**(2): 519-528.
Darbellay, F., C. Bochaton, L. Lopez-Delisle, B. Mascrez, P. Tschopp, S. Delpretti, J. Zakany and D. Duboule (2019). "The constrained architecture of mammalian Hox gene clusters." Proc Natl Acad Sci U S A **116**(27): 13424-13433.
Davis, A. P., D. P. Witte, H. M. Hsieh-Li, S. S. Potter and M. R. Capecchi (1995). "Absence of radius and ulna in mice lacking hoxa-11 and hoxd-11." Nature **375**(6534): 791-795.
Debnath, S., A. R. Yallowitz, J. McCormick, S. Lalani, T. Zhang, R. Xu, N. Li, Y. Liu, Y. S. Yang, M. Eiseman, J. H. Shim, M. Hameed, J. H. Healey, M. P. Bostrom, D. A. Landau and M. B. Greenblatt (2018). "Discovery of a periosteal stem cell mediating intramembranous bone formation." Nature **562**(7725): 133-139.
Deschamps, J. and J. van Nes (2005). "Developmental regulation of the Hox genes during axial morphogenesis in the mouse." Development **132**(13): 2931-2942.
Dobreva, G., M. Chahrour, M. Dautzenberg, L. Chirivella, B. Kanzler, I. Farinas, G. Karsenty and R. Grosschedl (2006). "SATB2 is a multifunctional determinant of craniofacial patterning and osteoblast differentiation." Cell **125**(5): 971-986.
Duchamp de Lageneste, O., A. Julien, R. Abou-Khalil, G. Frangi, C. Carvalho, N. Cagnard, C. Cordier, S. J. Conway and C. Colnot (2018). "Periosteum contains skeletal stem cells with high bone regenerative potential controlled by Periostin." Nat Commun **9**(1): 773.
Favier, B. and P. Dolle (1997). "Developmental functions of mammalian Hox genes." Mol Hum Reprod **3**(2): 115-131.
Favier, B., F. M. Rijli, C. FromentalRamain, V. Fraulob, P. Chambon and P. Dolle (1996). "Functional cooperation between the non-paralogous genes Hoxa-10 and Hoxd-11 in the developing forelimb and axial skeleton." Development **122**(2): 449-460.
Ferretti, C. and M. Mattioli-Belmonte (2014). "Periosteum derived stem cells for regenerative medicine proposals: Boosting current knowledge." World J Stem Cells **6**(3): 266-277.
Fuller, J. F., J. McAdara, Y. Yaron, M. Sakaguchi, J. K. Fraser and J. C. Gasson (1999). "Characterization of HOX gene expression during myelopoiesis: role of HOX A5 in lineage commitment and maturation." Blood **93**(10): 3391-3400.
Gardiner, D. M. and S. V. Bryant (1996). "Molecular mechanisms in the control of limb regeneration: the role of homeobox genes." Int J Dev Biol **40**(4): 797-805.
Gaspar-Maia, A., A. Alajem, E. Meshorer and M. Ramalho-Santos (2011). "Open chromatin in pluripotency and reprogramming." Nat Rev Mol Cell Biol **12**(1): 36-47.
Gavalas, A., M. Studer, A. Lumsden, F. M. Rijli, R. Krumlauf and P. Chambon (1998). "Hoxa1 and Hoxb1 synergize in patterning the hindbrain, cranial nerves and second pharyngeal arch." Development **125**(6): 1123-1136.
Gerber, T., P. Murawala, D. Knapp, W. Masselink, M. Schuez, S. Hermann, M. Gac-Santel, S. Nowoshilow, J. Kageyama, S. Khattak, J. D. Currie, J. G. Camp, E. M. Tanaka and B. Treutlein (2018). "Single-cell analysis uncovers convergence of cell identities during axolotl limb regeneration." Science **362**(6413).
Gruber, R., H. Koch, B. A. Doll, F. Tegtmeier, T. A. Einhorn and J. O. Hollinger (2006). "Fracture healing in the elderly patient." Exp Gerontol **41**(11): 1080-1093.

Gupta, P. B., C. M. Fillmore, G. Jiang, S. D. Shapira, K. Tao, C. Kuperwasser and E. S. Lander (2011). "Stochastic state transitions give rise to phenotypic equilibrium in populations of cancer cells." Cell **146**(4): 633-644.
Harris, A. M., P. L. Althausen, J. Kellam, M. J. Bosse, R. Castillo and G. Lower Extremity Assessment Project Study (2009). "Complications following limb-threatening lower extremity trauma." J Orthop Trauma **23**(1): 1-6.
Hassan, M. Q., R. Tare, S. H. Lee, M. Mandeville, B. Weiner, M. Montecino, A. J. van Wijnen, J. L. Stein, G. S. Stein and J. B. Lian (2007). "HOXA10 controls osteoblastogenesis by directly activating bone regulatory and phenotypic genes." Mol Cell Biol **27**(9): 3337-3352.
Hedlund, E., S. L. Karsten, L. Kudo, D. H. Geschwind and E. M. Carpenter (2004). "Identification of a Hoxd10-regulated transcriptional network and combinatorial interactions with Hoxa10 during spinal cord development." J Neurosci Res **75**(3): 307-319.
Houlihan, D. D., Y. Mabuchi, S. Morikawa, K. Niibe, D. Araki, S. Suzuki, H. Okano and Y. Matsuzaki (2012). "Isolation of mouse mesenchymal stem cells on the basis of expression of Sca-1 and PDGFR-alpha." Nat Protoc **7**(12): 2103-2111.
Hwang, J. H., O. S. Seok, H. R. Song, J. Y. Jo and J. K. Lee (2009). "HOXC10 as a Potential Marker for Discriminating between Amnion- and Decidua-Derived Mesenchymal Stem Cells." Cloning and Stem Cells **11**(2): 269-279.
Iyyanar, P. P. R. and A. J. Nazarali (2017). "Hoxa2 Inhibits Bone Morphogenetic Protein Signaling during Osteogenic Differentiation of the Palatal Mesenchyme." Front Physiol **8**: 929.
Izpisua-Belmonte, J. C., H. Falkenstein, P. Dolle, A. Renucci and D. Duboule (1991). "Murine genes related to the Drosophila AbdB homeotic genes are sequentially expressed during development of the posterior part of the body." EMBO J **10**(8): 2279-2289.
Josephson, A. M., V. Bradaschia-Correa, S. Lee, K. Leclerc, K. S. Patel, E. Muinos Lopez, H. P. Litwa, S. S. Neibart, M. Kadiyala, M. Z. Wong, M. M. Mizrahi, N. L. Yim, A. J. Ramme, K. A. Egol and P. Leucht (2019). "Age-related inflammation triggers skeletal stem/progenitor cell dysfunction." Proc Natl Acad Sci U S A **116**(14): 6995-7004.
Kalajzic, I., Z. Kalajzic, M. Kaliterna, G. Gronowicz, S. H. Clark, A. C. Lichtler and D. Rowe (2002). "Use of type I collagen green fluorescent protein transgenes to identify subpopulations of cells at different stages of the osteoblast lineage." Journal of Bone and Mineral Research **17**(1): 15-25.
Kalkan, T., N. Olova, M. Roode, C. Mulas, H. J. Lee, I. Nett, H. Marks, R. Walker, H. G. Stunnenberg, K. S. Lilley, J. Nichols, W. Reik, P. Bertone and A. Smith (2017). "Tracking the embryonic stem cell transition from ground state pluripotency." Development **144**(7): 1221-1234.
Kang, S. G., H. Chung, Y. D. Yoo, J. G. Lee, Y. I. Choi and Y. S. Yu (2001). "Mechanism of growth inhibitory effect of Mitomycin-C on cultured human retinal pigment epithelial cells: apoptosis and cell cycle arrest." Curr Eye Res **22**(3): 174-181.
Kanzler, B., S. J. Kuschert, Y. H. Liu and M. Mallo (1998). "Hoxa-2 restricts the chondrogenic domain and inhibits bone formation during development of the branchial area." Development **125**(14): 2587-2597.
Kmita, M., B. Tarchini, J. Zakany, M. Logan, C. J. Tabin and D. Duboule (2005). "Early developmental arrest of mammalian limbs lacking HoxA/HoxD gene function." Nature **435**(7045): 1113-1116.
Krumlauf, R. (1994). "Hox genes in vertebrate development." Cell **78**(2): 191-201.

Kwong, F. N. and M. B. Harris (2008). "Recent developments in the biology of fracture repair." J Am Acad Orthop Surg **16**(11): 619-625.
Lawrence, H. J., J. Christensen, S. Fong, Y. L. Hu, I. Weissman, G. Sauvageau, R. K. Humphries and C. Largman (2005). "Loss of expression of the Hoxa-9 homeobox gene impairs the proliferation and repopulating ability of hematopoietic stem cells." Blood **106**(12): 3988-3994.
Lawrence, H. J., G. Sauvageau, R. K. Humphries and C. Largman (1996). "The role of HOX homeobox genes in normal and leukemic hematopoiesis." Stem Cells **14**(3): 281-291.
Leucht, P., J. B. Kim, R. Amasha, A. W. James, S. Girod and J. A. Helms (2008). "Embryonic origin and Hox status determine progenitor cell fate during adult bone regeneration." Development **135**(17): 2845-2854.
Liedtke, S., A. Buchheiser, J. Bosch, F. Bosse, F. Kruse, X. Y. Zhao, S. Santourlidis and G. Kogler (2010). "The HOX Code as a "biological fingerprint" to distinguish functionally distinct stem cell populations derived from cord blood." Stem Cell Research **5**(1): 40-50.
Lin, T. Y., T. Gerber, Y. Taniguchi-Sugiura, P. Murawala, S. Hermann, L. Grosser, E. Shibata, B. Treutlein and E. M. Tanaka (2021). "Fibroblast dedifferentiation as a determinant of successful regeneration." Dev Cell **56**(10): 1541-1551 e1546.
Lovato, T. L., T. P. Nguyen, M. R. Molina and R. M. Cripps (2002). "The Hox gene abdominal-A specifies heart cell fate in the Drosophila dorsal vessel." Development **129**(21): 5019-5027.
Mabuchi, Y., C. Okawara, S. Mendez-Ferrer and C. Akazawa (2021). "Cellular Heterogeneity of Mesenchymal Stem/Stromal Cells in the Bone Marrow." Front Cell Dev Biol **9**: 689366.
Magli, M. C., C. Largman and H. J. Lawrence (1997). "Effects of HOX homeobox genes in blood cell differentiation." J Cell Physiol **173**(2): 168-177.
Magnusson, M., A. C. Brun, N. Miyake, J. Larsson, M. Ehinger, J. M. Bjornsson, A. Wutz, M. Sigvardsson and S. Karlsson (2007). "HOXA10 is a critical regulator for hematopoietic stem cells and erythroid/megakaryocyte development." Blood **109**(9): 3687-3696.
Mark, M., T. Lufkin, J. L. Vonesch, E. Ruberte, J. C. Olivo, P. Dolle, P. Gorry, A. Lumsden and P. Chambon (1993). "Two rhombomeres are altered in Hoxa-1 mutant mice." Development **119**(2): 319-338.
McNulty, C. L., J. N. Peres, N. Bardine, W. M. van den Akker and A. J. Durston (2005). "Knockdown of the complete Hox paralogous group 1 leads to dramatic hindbrain and neural crest defects." Development **132**(12): 2861-2871.
Mizoguchi, T., S. Pinho, J. Ahmed, Y. Kunisaki, M. Hanoun, A. Mendelson, N. Ono, H. M. Kronenberg and P. S. Frenette (2014). "Osterix marks distinct waves of primitive and definitive stromal progenitors during bone marrow development." Dev Cell **29**(3): 340-349.
Morikawa, S., Y. Mabuchi, Y. Kubota, Y. Nagai, K. Niibe, E. Hiratsu, S. Suzuki, C. Miyauchi-Hara, N. Nagoshi, T. Sunabori, S. Shimmura, A. Miyawaki, T. Nakagawa, T. Suda, H. Okano and Y. Matsuzaki (2009). "Prospective identification, isolation, and systemic transplantation of multipotent mesenchymal stem cells in murine bone marrow." J Exp Med **206**(11): 2483-2496.
Morris, S. A. (2016). "Direct lineage reprogramming via pioneer factors; a detour through developmental gene regulatory networks." Development **143**(15): 2696-2705.
Nieminen, S., M. Nurmi and K. Satokari (1981). "Healing of femoral neck fractures; influence of fracture reduction and age." Ann Chir Gynaecol **70**(1): 26-31.

Nilsson, B. E. and P. Edwards (1969). "Age and fracture healing: a statistical analysis of 418 cases of tibial shaft fractures." Geriatrics **24**(2): 112-117.
Nogi, T. and K. Watanabe (2001). "Position-specific and non-colinear expression of the planarian posterior (Abdominal-B-like) gene." Dev Growth Differ **43**(2): 177-184.
Orii, H., K. Kato, Y. Umesono, T. Sakurai, K. Agata and K. Watanabe (1999). "The planarian HOM/HOX homeobox genes (Plox) expressed along the anteroposterior axis." Dev Biol **210**(2): 456-468.
Owens, B. M. and R. G. Hawley (2002). "HOX and non-HOX homeobox genes in leukemic hematopoiesis." Stem Cells **20**(5): 364-379.
Papageorgiou, S. (2012). "Comparison of models for the collinearity of hox genes in the developmental axes of vertebrates." Curr Genomics **13**(3): 245-251.
Pineault, K. M., J. Y. Song, K. M. Kozloff, D. Lucas and D. M. Wellik (2019). "Hox11 expressing regional skeletal stem cells are progenitors for osteoblasts, chondrocytes and adipocytes throughout life." Nat Commun **10**(1): 3168.
Pineault, N., C. D. Helgason, H. J. Lawrence and R. K. Humphries (2002). "Differential expression of Hox, Meis1, and Pbx1 genes in primitive cells throughout murine hematopoietic ontogeny." Exp Hematol **30**(1): 49-57.
Pinho, S., J. Lacombe, M. Hanoun, T. Mizoguchi, I. Bruns, Y. Kunisaki and P. S. Frenette (2013). "PDGFRalpha and CD51 mark human nestin+ sphere-forming mesenchymal stem cells capable of hematopoietic progenitor cell expansion." J Exp Med **210**(7): 1351-1367.
Roberts, S. J., L. Geris, G. Kerckhofs, E. Desmet, J. Schrooten and F. P. Luyten (2011). "The combined bone forming capacity of human periosteal derived cells and calcium phosphates." Biomaterials **32**(19): 4393-4405.
Roberts, S. J., N. van Gastel, G. Carmeliet and F. P. Luyten (2015). "Uncovering the periosteum for skeletal regeneration: the stem cell that lies beneath." Bone **70**: 10-18.
Rossel, M. and M. R. Capecchi (1999). "Mice mutant for both Hoxa1 and Hoxb1 show extensive remodeling of the hindbrain and defects in craniofacial development." Development **126**(22): 5027-5040.
Rux, D. R., J. Y. Song, I. T. Swinehart, K. M. Pineault, A. J. Schlientz, K. G. Trulik, S. A. Goldstein, K. M. Kozloff, D. Lucas and D. M. Wellik (2016). "Regionally Restricted Hox Function in Adult Bone Marrow Multipotent Mesenchymal Stem/Stromal Cells." Dev Cell **39**(6): 653-666.
Rux, D. R. and D. M. Wellik (2017). "Hox genes in the adult skeleton: Novel functions beyond embryonic development." Dev Dyn **246**(4): 310-317.
Sakaguchi, Y., I. Sekiya, K. Yagishita and T. Muneta (2005). "Comparison of human stem cells derived from various mesenchymal tissues: superiority of synovium as a cell source." Arthritis Rheum **52**(8): 2521-2529.
Sauvageau, G., U. Thorsteinsdottir, C. J. Eaves, H. J. Lawrence, C. Largman, P. M. Lansdorp and R. K. Humphries (1995). "Overexpression of HOXB4 in hematopoietic cells causes the selective expansion of more primitive populations in vitro and in vivo." Genes Dev **9**(14): 1753-1765.
Schiedlmeier, B., H. Klump, E. Will, G. Arman-Kalcek, Z. Li, Z. Wang, A. Rimek, J. Friel, C. Baum and W. Ostertag (2003). "High-level ectopic HOXB4 expression confers a profound in vivo competitive growth advantage on human cord blood CD34+ cells, but impairs lymphomyeloid differentiation." Blood **101**(5): 1759-1768.

Sela, Y., N. Molotski, S. Golan, J. Itskovitz-Eldor and Y. Soen (2012). "Human embryonic stem cells exhibit increased propensity to differentiate during the G1 phase prior to phosphorylation of retinoblastoma protein." Stem Cells **30**(6): 1097-1108.
Shen, W. F., J. C. Montgomery, S. Rozenfeld, J. J. Moskow, H. J. Lawrence, A. M. Buchberg and C. Largman (1997). "AbdB-like Hox proteins stabilize DNA binding by the Meis1 homeodomain proteins." Mol Cell Biol **17**(11): 6448-6458.
Shen, W. F., S. Rozenfeld, H. J. Lawrence and C. Largman (1997). "The Abd-B-like Hox homeodomain proteins can be subdivided by the ability to form complexes with Pbx1a on a novel DNA target." J Biol Chem **272**(13): 8198-8206.
Small, K. M. and S. S. Potter (1993). "Homeotic transformations and limb defects in Hox A11 mutant mice." Genes Dev **7**(12A): 2318-2328.
Song, J. Y., K. M. Pineault, J. M. Dones, R. T. Raines and D. M. Wellik (2020). "Hox genes maintain critical roles in the adult skeleton." Proc Natl Acad Sci U S A.
Studer, M., A. Lumsden, L. Ariza-McNaughton, A. Bradley and R. Krumlauf (1996). "Altered segmental identity and abnormal migration of motor neurons in mice lacking Hoxb-1." Nature **384**(6610): 630-634.
Taghon, T., F. Stolz, M. De Smedt, M. Cnockaert, B. Verhasselt, J. Plum and G. Leclercq (2002). "HOX-A10 regulates hematopoietic lineage commitment: evidence for a monocyte-specific transcription factor." Blood **99**(4): 1197-1204.
Tapias, A., Z. W. Zhou, Y. Shi, Z. Chong, P. Wang, M. Groth, M. Platzer, W. Huttner, Z. Herceg, Y. G. Yang and Z. Q. Wang (2014). "Trrap-dependent histone acetylation specifically regulates cell-cycle gene transcription to control neural progenitor fate decisions." Cell Stem Cell **14**(5): 632-643.
Tarchini, B. and D. Duboule (2006). "Control of Hoxd genes' collinearity during early limb development." Dev Cell **10**(1): 93-103.
Thorsteinsdottir, U., A. Mamo, E. Kroon, L. Jerome, J. Bijl, H. J. Lawrence, K. Humphries and G. Sauvageau (2002). "Overexpression of the myeloid leukemia-associated Hoxa9 gene in bone marrow cells induces stem cell expansion." Blood **99**(1): 121-129.
Thorsteinsdottir, U., G. Sauvageau, M. R. Hough, W. Dragowska, P. M. Lansdorp, H. J. Lawrence, C. Largman and R. K. Humphries (1997). "Overexpression of HOXA10 in murine hematopoietic cells perturbs both myeloid and lymphoid differentiation and leads to acute myeloid leukemia." Mol Cell Biol **17**(1): 495-505.
Thummel, R., M. Ju, M. P. Sarras and A. R. Godwin (2007). "Both Hoxc13 orthologs are functionally important for zebrafish tail fin regeneration." Development Genes and Evolution **217**(6): 413-420.
Ugarte, F., R. Sousae, B. Cinquin, E. W. Martin, J. Krietsch, G. Sanchez, M. Inman, H. Tsang, M. Warr, E. Passegue, C. A. Larabell and E. C. Forsberg (2015). "Progressive Chromatin Condensation and H3K9 Methylation Regulate the Differentiation of Embryonic and Hematopoietic Stem Cells." Stem Cell Reports **5**(5): 728-740.
van den Akker, E., M. Reijnen, J. Korving, A. Brouwer, F. Meijlink and J. Deschamps (1999). "Targeted inactivation of Hoxb8 affects survival of a spinal ganglion and causes aberrant limb reflexes." Mech Dev **89**(1-2): 103-114.
van Gastel, N., S. Torrekens, S. J. Roberts, K. Moermans, J. Schrooten, P. Carmeliet, A. Luttun, F. P. Luyten and G. Carmeliet (2012). "Engineering vascularized bone: osteogenic and proangiogenic potential of murine periosteal cells." Stem Cells **30**(11): 2460-2471.

Wahba, G. M., S. L. Hostikka and E. M. Carpenter (2001). "The paralogous Hox genes Hoxa10 and Hoxd10 interact to pattern the mouse hindlimb peripheral nervous system and skeleton." Dev Biol **231**(1): 87-102.
Wang, W., Y. Quan, Q. Fu, Y. Liu, Y. Liang, J. Wu, G. Yang, C. Luo, Q. Ouyang and Y. Wang (2014). "Dynamics between cancer cell subpopulations reveals a model coordinating with both hierarchical and stochastic concepts." PLoS One **9**(1): e84654.
Wellik, D. M. and M. R. Capecchi (2003). "Hox10 and Hox11 genes are required to globally pattern the mammalian skeleton." Science **301**(5631): 363-367.
Wosczyna, M. N., C. T. Konishi, E. E. Perez Carbajal, T. T. Wang, R. A. Walsh, Q. Gan, M. W. Wagner and T. A. Rando (2019). "Mesenchymal Stromal Cells Are Required for Regeneration and Homeostatic Maintenance of Skeletal Muscle." Cell Rep **27**(7): 2029-2035 e2025.
Yang, Y. K., C. R. Ogando, C. Wang See, T. Y. Chang and G. A. Barabino (2018). "Changes in phenotype and differentiation potential of human mesenchymal stem cells aging in vitro." Stem Cell Res Ther **9**(1): 131.
Yoshimura, H., T. Muneta, A. Nimura, A. Yokoyama, H. Koga and I. Sekiya (2007). "Comparison of rat mesenchymal stem cells derived from bone marrow, synovium, periosteum, adipose tissue, and muscle." Cell Tissue Res **327**(3): 449-462.
Yue, R., B. O. Zhou, I. S. Shimada, Z. Zhao and S. J. Morrison (2016). "Leptin Receptor Promotes Adipogenesis and Reduces Osteogenesis by Regulating Mesenchymal Stromal Cells in Adult Bone Marrow." Cell Stem Cell **18**(6): 782-796.
Zanatta, A., A. M. Rocha, F. M. Carvalho, R. M. Pereira, H. S. Taylor, E. L. Motta, E. C. Baracat and P. C. Serafini (2010). "The role of the Hoxa10/HOXA10 gene in the etiology of endometriosis and its related infertility: a review." J Assist Reprod Genet **27**(12): 701-710.
Zhou, B. O., R. Yue, M. M. Murphy, J. G. Peyer and S. J. Morrison (2014). "Leptin-receptor-expressing mesenchymal stromal cells represent the main source of bone formed by adult bone marrow." Cell stem cell **15**(2): 154-168.

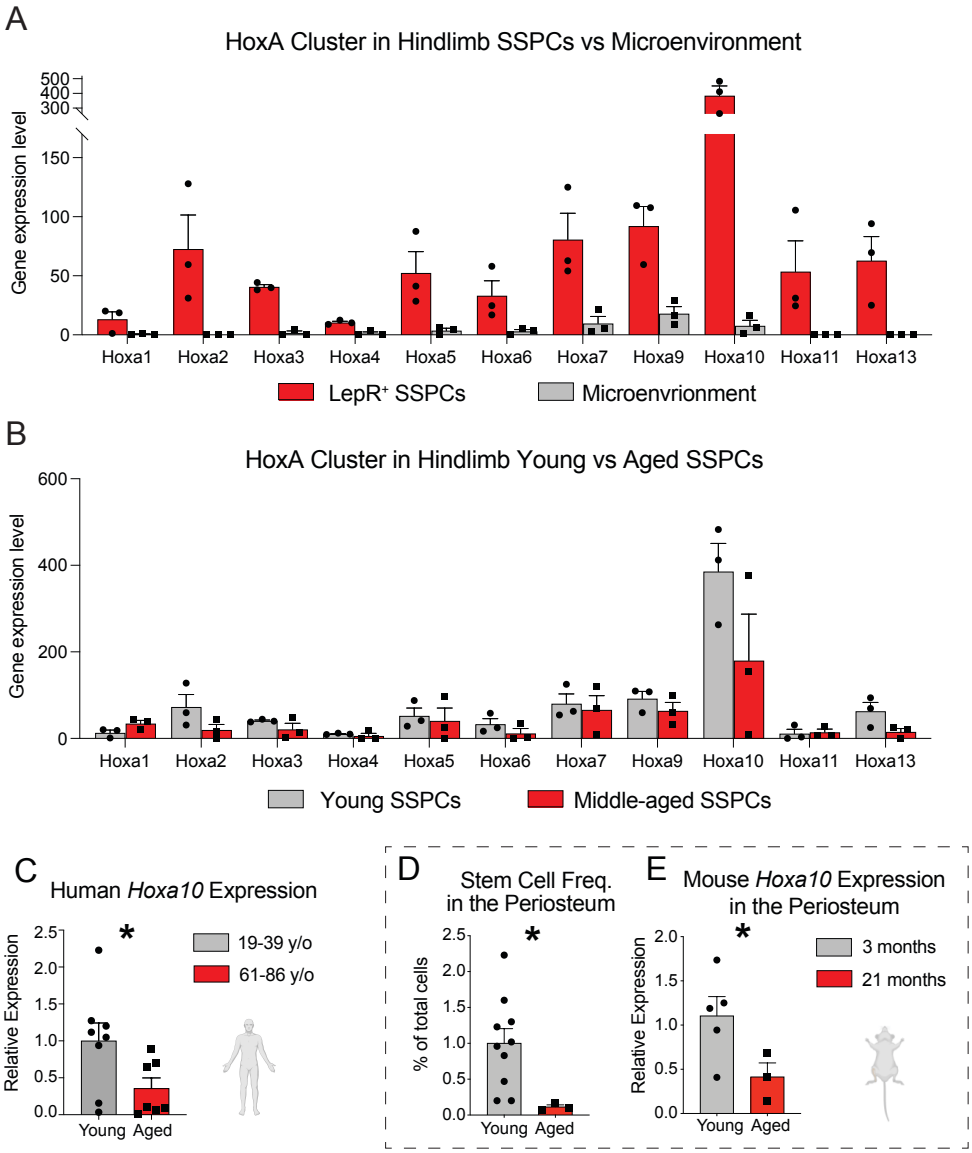

Figure 1. Hox gene expression is enriched in skeletal stem/ progenitor cells and declines with age. (**A**) RNA-sequencing revealed the gene expression pattern for 11 HoxA cluster genes in $CD45^{-}Ter119^{-}CD31^{-}LepR+$ SSPCs or cells of the microenvironment harvested from 12-week-old, freshly-isolated tibiae and femurs. HoxA genes are highly enriched in the SSPC population and *Hoxa10*, with the most normalized reads, is the most highly expressed. $n = 3$. (**B**) RNA-sequencing determined the gene expression levels of HoxA cluster genes in young, 12-week-old $CD45^{-}Ter119^{-}CD31^{-}LepR+$ SSPCs versus those of middle-aged, 52-week-old SSPCs. $n = 3$. (**C**) The relative expression of Hoxa10 in bone marrow samples harvested from the fracture sites of young (18-39 years-old) and aged (61-86 years-old) human patients, as measured by qRT-PCR. $n = 8$ (young), $n = 7$ (aged). (**D** and **E**) When tibial periosteal cell were harvested from young (3-month-old) and aged (21-month-old) mice, flow cytometry revealed the frequency of $6C3^{-}CD90^{-}CD49f^{low}CD51^{low}CD200^{+}CD105^{-}$ periosteal stem cells (**D**) and qRT-PCR determined the relative expression of Hoxa10 (**E**). $n = 10$ (young, flow cytometry), $n = 5$ (young, qRT-PCR), $n = 3$ (aged). $^{*}p < 0.05$. Two tailed Student's t-test. Error bars are SEM.

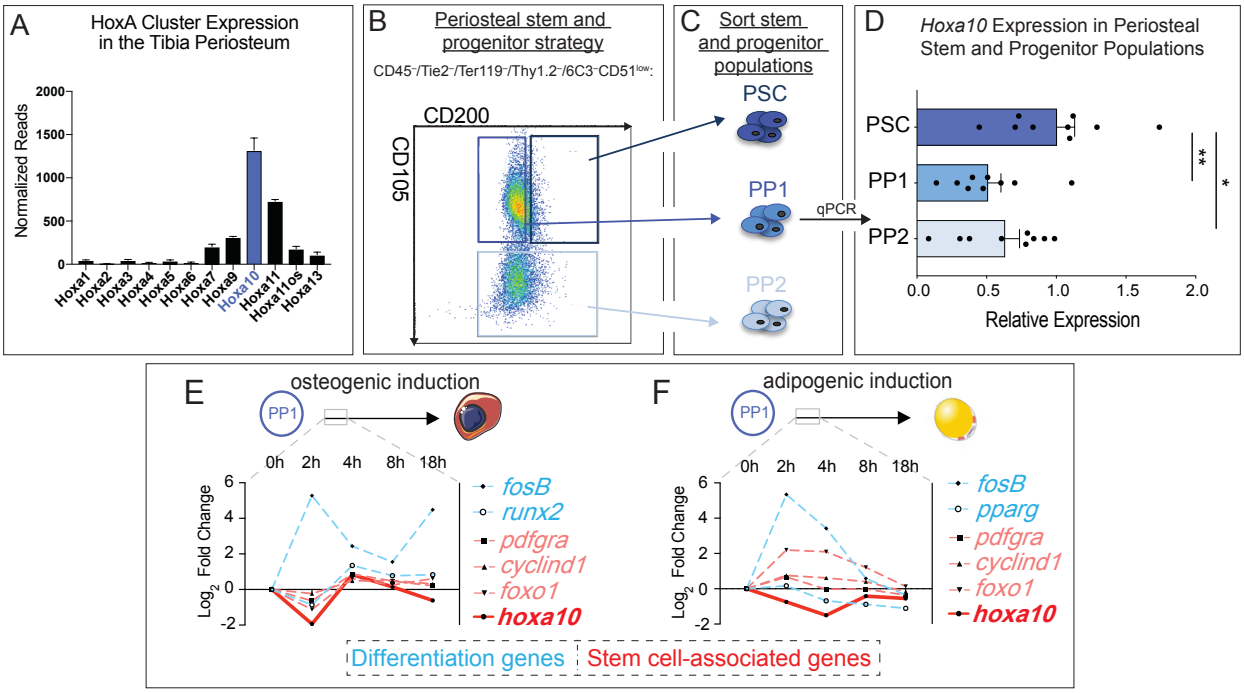

Figure 2. Hoxa10 is the most highly expressed Hox gene in tibial periosteal cells. (**A**) RNAseq gene expression data of the HoxA cluster derived from 12-week-old tibial periosteal cells. (**B**) Sample FACS plot of periosteal stem and progenitor cells as defined by *Debnath et al., 2018* and (**C**) strategy for isolating periosteal stem cells (PSC), periosteal progenitor 1 (PP1) cells, and periosteal progenitor 2 (PP2) cells. (**D**) The relative gene expression of *Hoxa10* in freshly isolated stem and progenitor populations of tibial periosteum as measured by qRT-PCR. n = 3 mice. (**E,F**) The gene expression of multiple skeletal stem cell and differentiation genes during an 18h *in vitro* time course of osteogenic (**E**) or adipogenic (**F**) induction relative to growth media controls. n = 3. *$p < 0.05$, **$p < 0.01$. Two tailed Student's t-test. Error bars are SEM.

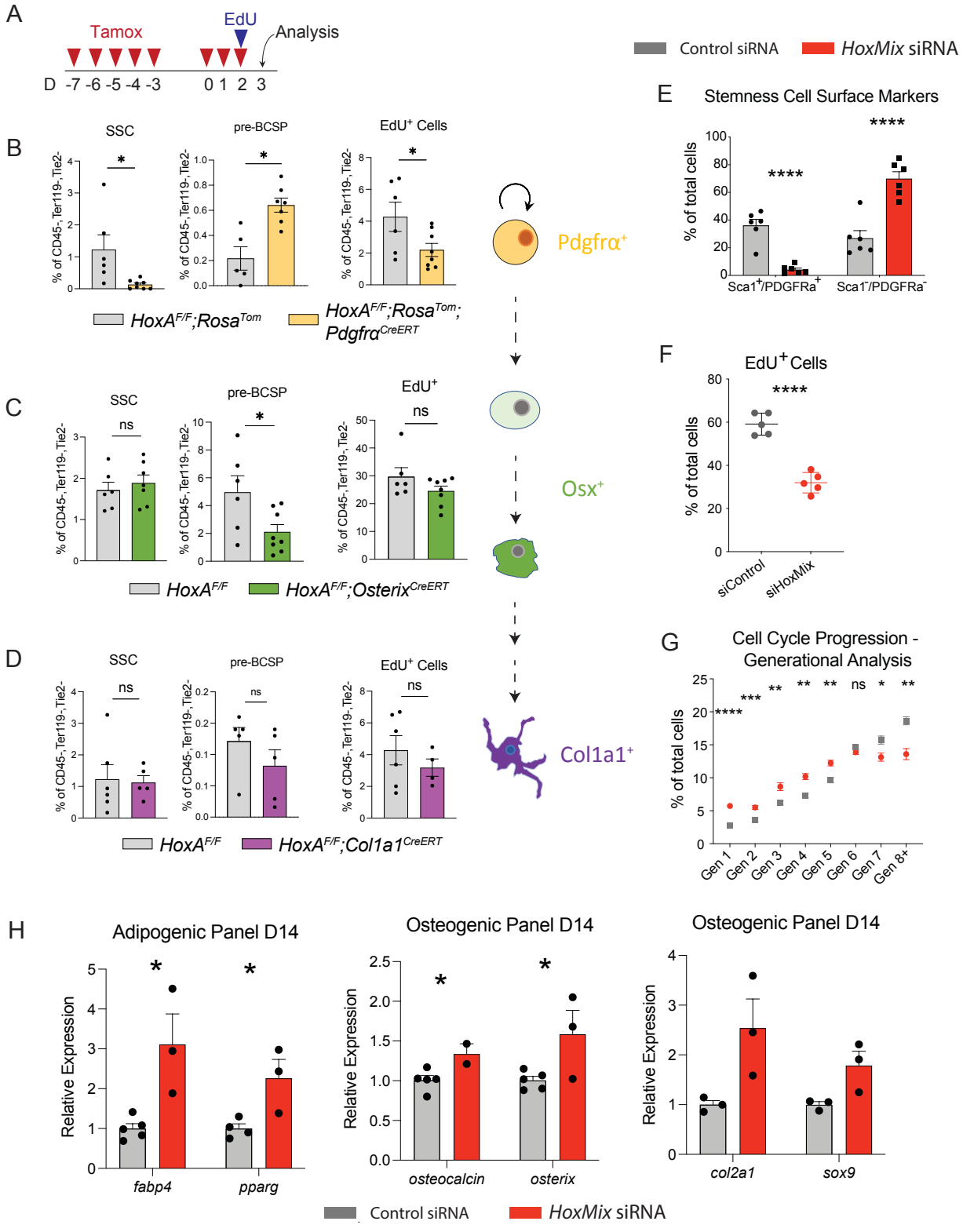

Figure 3. Inhibition of Hox genes in stem and progenitor cells triggers a loss of skeletal stem cells and periosteal stemness properties. (**A**) Scheme of tamoxifen dosing protocol (2mg/day) and EdU administration. (**B**-**D**) Flow cytometry revealed the percentage of $6C3^{-}CD90^{-}CD51^{+}CD200^{+}CD105^{-}$ skeletal stem cells, $6C3^{-}CD90^{-}CD51^{+}CD200^{-}CD105^{-}$ pre-Bone/Chondro/Stromal progenitors (pre-BCSPs), and EdU^{+} proliferative cells in the nonhematopoietic compartment of $Pdgfr\alpha^{CreERT};HoxA^{flox/flox}$ (**B**), $Osterix^{CreERT};HoxA^{flox/flox}$ (**C**), and $Col1a1^{CreERT};HoxA^{flox/flox}$ (**D**) and $HoxA^{flox/flox}$ control mice. (**E**-**F**) Simultaneous knockdown of *Hoxa10*, *Hoxa11*, *Hoxd10*, *Hoxd11*, and *Hoxc10* (*HoxMix*) was used to test the extent of stem cell potency in Hox-deficient tbial PSPCs. (**E**) After 7 days of control and *HoxMix* siRNA, PSPCs were analyzed for stemness-associated cell surface marker expression using flow cytometry. $n = 3$ each condition. (**F**) PSPCs were pulsed with EdU for 15 hours following HoxMix and nontargeting control siRNA knockdown; the amount of EdU-positive cells was then measured by flow cytometry. $n = 5$. (**G**) siControl and si*HoxMix* tibial PSPCs were also treated with Cell Trace™ and subjected to flow cytometry to categorize cells by generation after six days of incubation. $n = 5$ (control), $n = 7$ (*HoxMix*). (**H**) Relative expression of adipogenic, osteogenic, and chondrogenic genes in tibial PSPCs serially transfected with control and *HoxMix* siRNA over the course of 14 days – measured by qRT-PCR. $n = 5$ (control), $n = 3$ (*HoxMix*). *ns* = not significant, $*p < 0.05$, $**p < 0.01$, $***p < 0.001$, $****p < 0.0001$. Two tailed Student's t-test. Error bars are SEM.

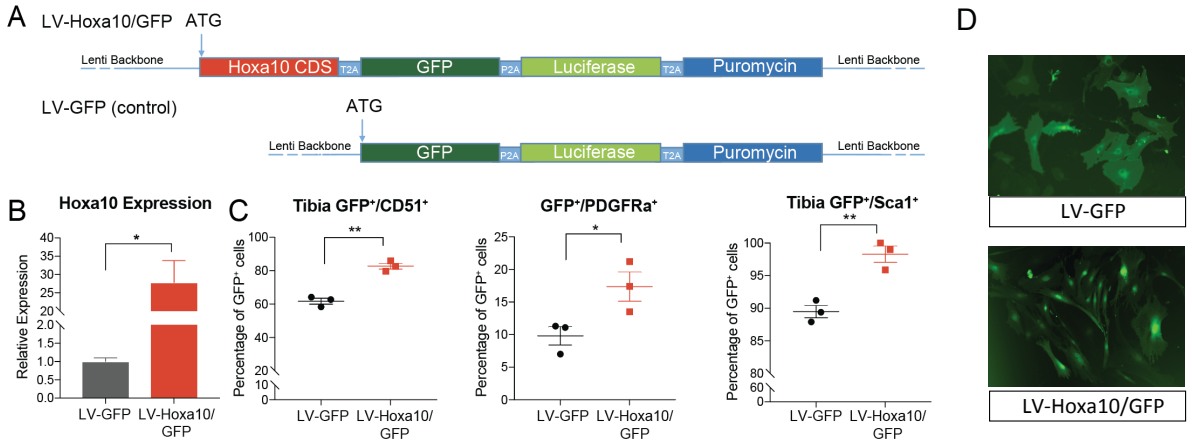

Figure 4. *Hoxa10* expression is sufficient to promote skeletal stem cell potency. (**A**) Schematic of lentiviral constructs used to transduce PSPCs. (**B**) qRT-PCR was used to reveal the relative expression of *Hoxa10* in control (LV-GFP) and *Hoxa10*-overexpressing (LV-Hoxa10/GFP) tibial PSPCs 11 days after infection. n = 3. (**C**) LV-GFP- and LV-Hoxa10/GFP-transduced tibial PSPCs were subjected to flow cytometry after a 7-day incubation to reveal the balance of infected GFP^+ cells exhibiting the skeletal stem cell surface markers CD51, PDGFRα, and SCA1. n =3. (**D**) GFP fluorescent images demonstrating both the stable expression of the GFP marker and cell morphological differences after 7 days in LV-GFP- and LV-Hoxa10/GFP-transduced tibial PSPCs. *$p < 0.05$, **$p < 0.01$. Two tailed Student's t-test. Error bars are SEM.

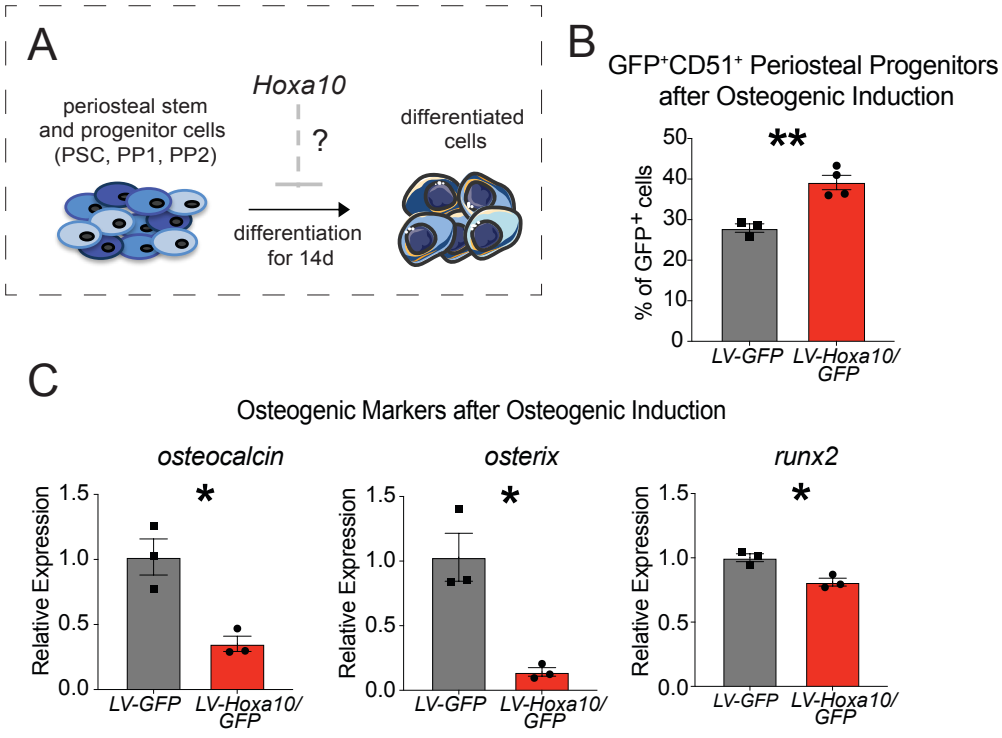

Figure 5. Hoxa10-overexpressing periosteal stem and progenitor cells display deficient osteodifferentiation. (**A**) Schematic of *in vitro* experiments performed in (**B**, **C**) to investigate whether *Hoxa10* overexpression can inhibit the differentiation of PSPCs after 14 days of osteogenic induction. (**B**) The balance of nonhematopoietic 6C3^{-}CD90^{-} CD51^{+}GFP^{+} PSPCs as a percentage of total infected cells (GFP^{+} cells) after transduction with *LV-GFP* or *LV-Hoxa10/GFP* and 14 days of osteoinduction media as measured by qRT-PCR. n = 3, *LV-GFP*; n = 4, *LV-Hoxa10/GFP* (**C**) Relative expression of osteogenic genes in *LV-GFP* or *LV-Hoxa10/GFP*-infected tibial periosteal stem and progenitors cells after a 14-day course of osteoinduction media. n = 3 each condition. *$p < 0.05$, **$p < 0.01$. Two tailed Student's t-test. Error bars are SEM.

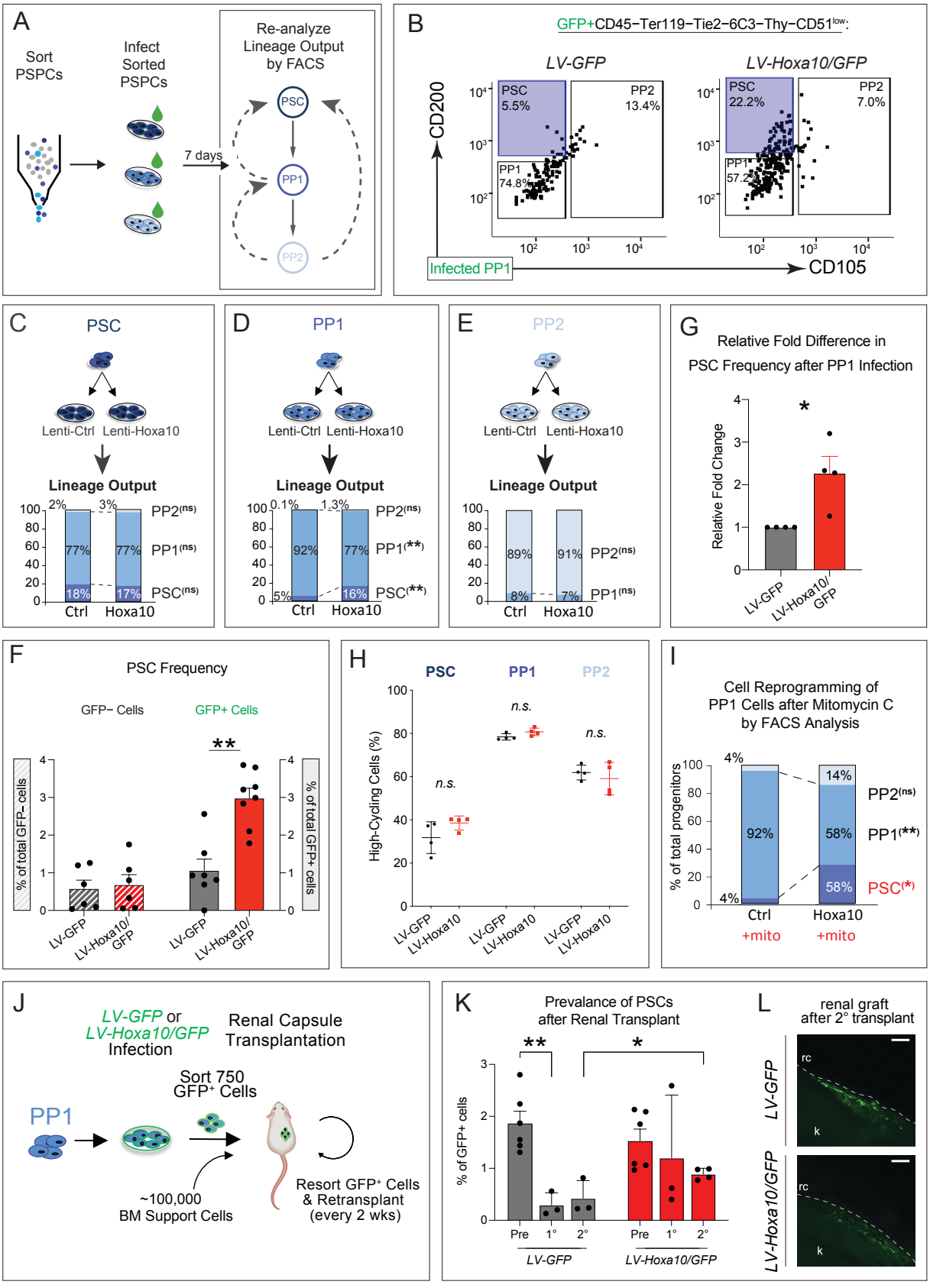

Figure 6. Hoxa10 overexpression mediates reprogramming of adult tibial PP1 cells into PSCs. (**A**) Experimental plan to test the reprogramming abilities of *Hoxa10.* Tibial PSCs, PP1 and PP2 cells were separately isolated by FACS. Each cell population was infected with *LV-GFP* or *LV-Hoxa10/GFP* and analyzed by flow cytometry after 7 days of incubation. (**B**) Representative FACS plots of the PSPC lineage output 7 days after transduction of PP1 cells with *LV-GFP* or *LV-Hoxa10/GFP*. Only infected (GFP^+) cells were evaluated. (**C**-**E**) Flow cytometric analysis of the distribution of GFP^+ PSCs, PP1, and PP2 cells within the $CD51^+$ stem and progenitor cell compartment 7 days after *LV-GFP* or *LV-Hoxa10/GFP* infection of PSCs (**C**), PP1 (**D**), and PP2 (**E**) cells. n = 3 (PSC), n = 3 (PP1), n = 5 (PP2). (**F**) The relative fold change in GFP^+ PSCs within the PSPC compartment after transduction of PP1 cells with *LV-GFP* or *LV-Hoxa10/GFP. n* = 4 separate experiments. (**G**) The frequency of PSCs among total cells 7 days after the infection of PP1 cells with *LV-GFP* or *LV-Hoxa10/GFP*. Uninfected (GFP^-) and infected (GFP^+) are shown separately. (**H**) *LV-GFP*- or *LV-Hoxa10/GFP*-infected tibial PSPCs were also treated with Cell Trace™ and subjected to flow cytometry to categorize cells as high- or low-cycling after six days of incubation. Gating strategy is presented in **Supplementary Fig. 3A**. n = 4 each condition. (**I**) Flow cytometry revealed the lineage hierarchy of tibial PP1 cells 7 days after 10ug/mL mitomycin C treatment and infection with *LV-GFP*- or *LV-Hoxa10/GFP. n* = 3. (**J**) Experimental plan to carry out serial transplants of reprogrammed periosteal cells under the renal capsule to test self-renewal capacity. (**K**) PP1 cells were first transduced with either *LV-GFP* or *LV-Hoxa10/GFP* and the prevalence of GFP-labelled PSCs was then assessed by flow cytometry before (Pre) and after each round of transplantation. n = 6, Pre-*LV-GFP* and Pre-*LV-Hoxa10/GFP*; n = 3, 1°-*LV-GFP* and 1°-*LV-Hoxa10/GFP*; n = 3, 2°-*LV-GFP*; n = 4, 2°-*LV-Hoxa10/GFP.* (**L**) Representative fluorescent images of renal capsule grafts derived from *LV-GFP* or *LV-Hoxa10/GFP*-infected periosteal cells after two rounds of transplantation (rc = renal capsule, k = kidney). Scale bars, 200 μm. (**B**-**E**, **G**) Complete results and statistics are provided in **Table 1.** *n.s.* = not significant, $*p < 0.05$, $**p < 0.01$. Two tailed Student's t-test. Error bars are SEM.

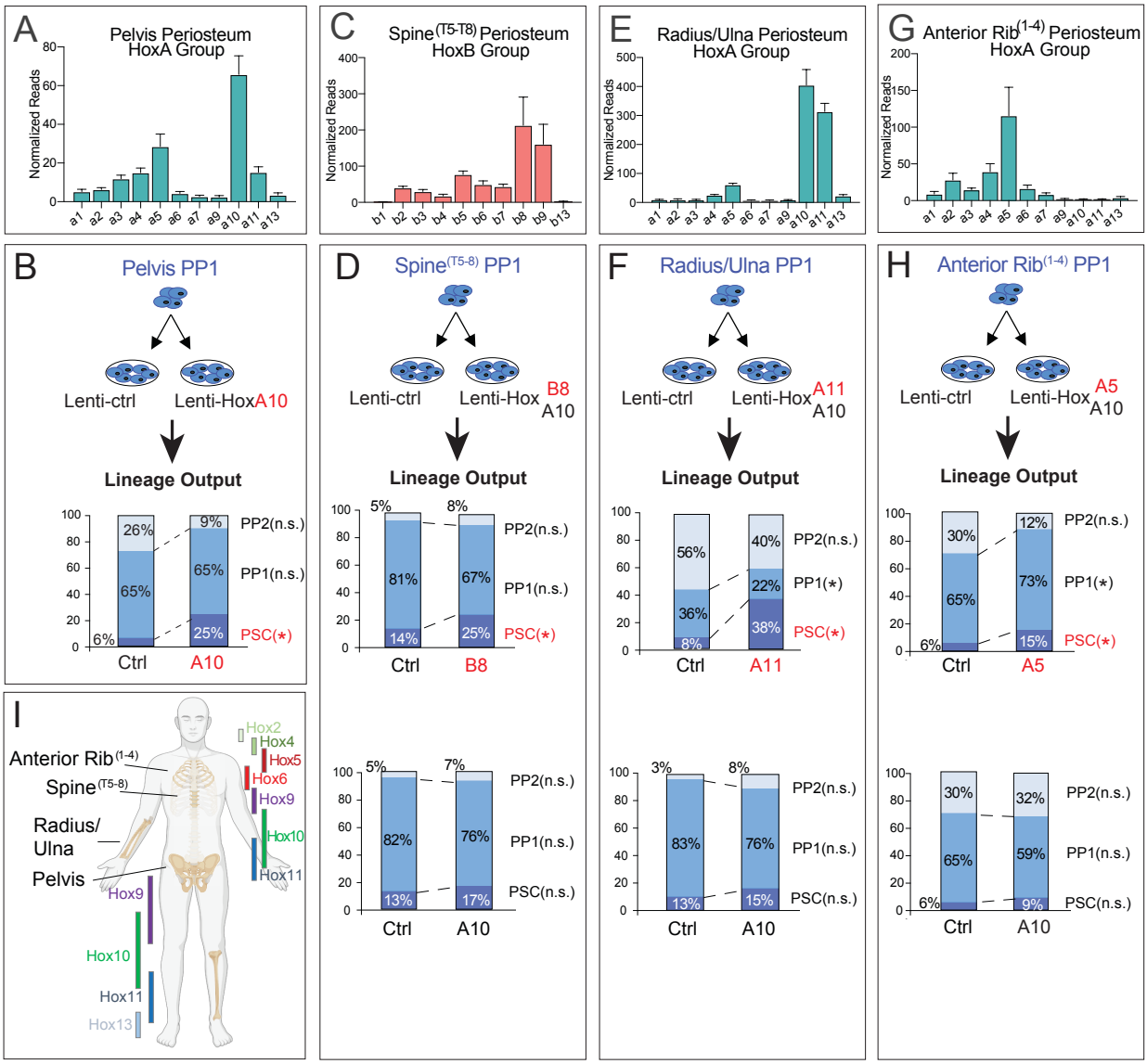

Figure 7. The regional specificity of *Hox* function is maintained in the adult skeleton. (**A, C, E, G**) The expression profile of the Hox cluster containing the highest expressed Hox gene in periosteal cells of the pelvis (**A**), spine$^{T5\text{-}T8}$ (**C**), radius/ulna (**E**), and anterior rib$^{1\text{-}4}$ (**G**). *n* = 4 mice for each skeletal element. Full Hox expression data in **Supplementary Fig. 6**. (**B**, **D**, **F**, **H**) The lineage output of stem and progenitors 7 days after infecting PP1 cells deriving from the pelvis (**B**), spine$^{T5\text{-}T8}$ (**D**), radius/ulna (**F**), and anterior rib$^{1\text{-}4}$ (**H**) with either *LV-Hoxa10/GFP*, *LV-Hoxb8/GFP* , *LV-Hoxa11/GFP, or LV-Hoxa5/GFP*, respectively – and with *LV-GFP* (Ctrl) and *LV-Hoxa10/GFP* serving as a control. *n* = 5, pelvis (Ctrl and A10); *n* = 4, spine (Ctrl and B8); *n* = 3, spine (Ctrl and A10); *n* = 4 and *n* = 5, radius/ulna (Ctrl and A11, respectively); *n* = 5, radius/ulna (Ctrl and A10); *n* =9, *n* = 8, and *n* = 9, anterior rib (Ctrl, A5, and A10, respectively). Full lineage output data and statistics are provided in **Table 2**. (**I**) Diagram of skeletal elements investigated along with the proposed regional restriction Hox expression in adult skeletal tissues (adapted from *Rux and Wellik, 2017*). *n.s.* = not significant, $*p < 0.05$. Two tailed Student's t-test. Error bars are SEM.

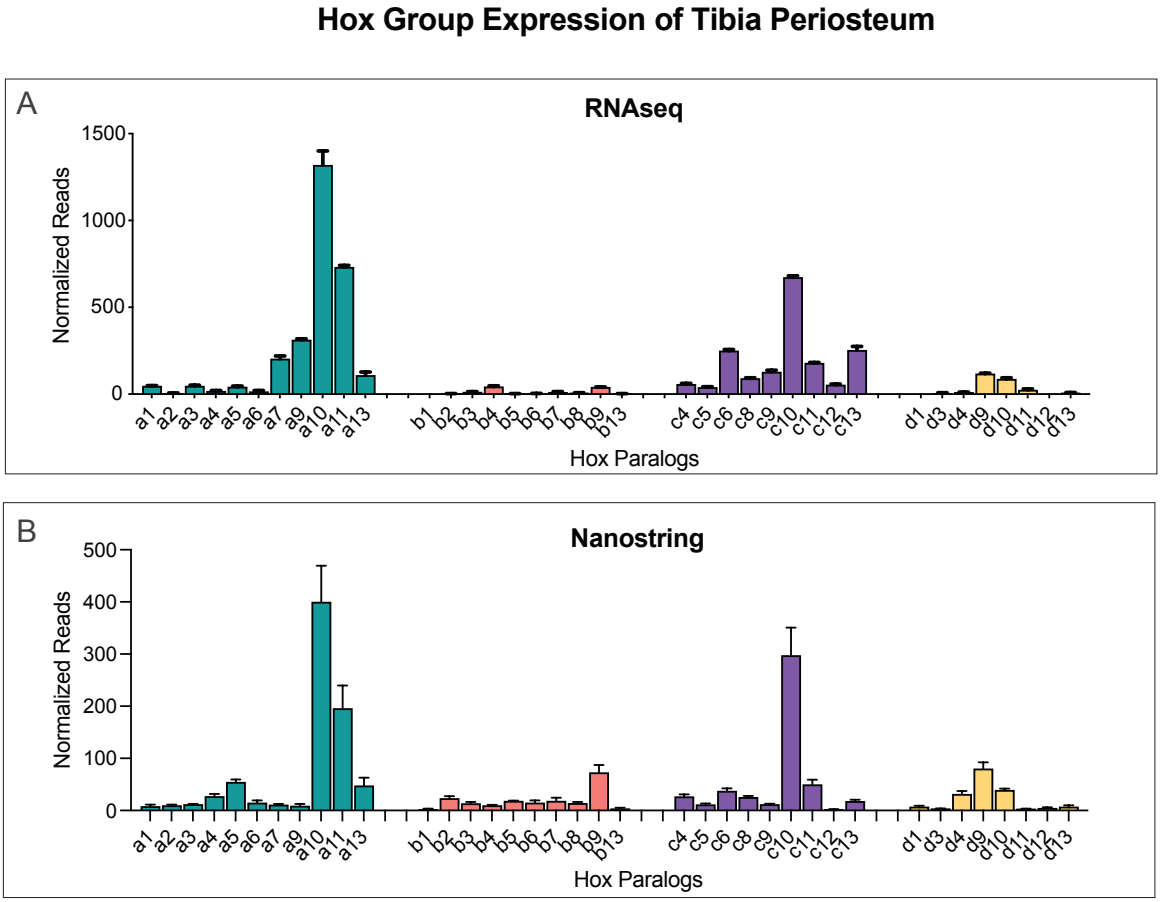

Supplementary Figure 1. *Hox* expression profile of adult tibia periosteum. (**A**). Bulk RNAseq revealed the gene expression pattern for all 39 Hox genes in 12-week-old, freshly-isolated tibial periosteum. *Hoxa10*, with the most normalized reads, is the most highly expressed. *n* = 3 mice. (**B**) Nanostring™ probes against all 39 Hox genes revealed their absolute expression profile in the adult tibia periosteum. *Hoxa10* contained the most normalized reads. *n* = 4 mice. (**C**) Representative FACS plot demonstrating the enrichment in PSPCs following 10 days of *in vitro* expansion of cells isolated from the periosteum. Error bars are SEM.

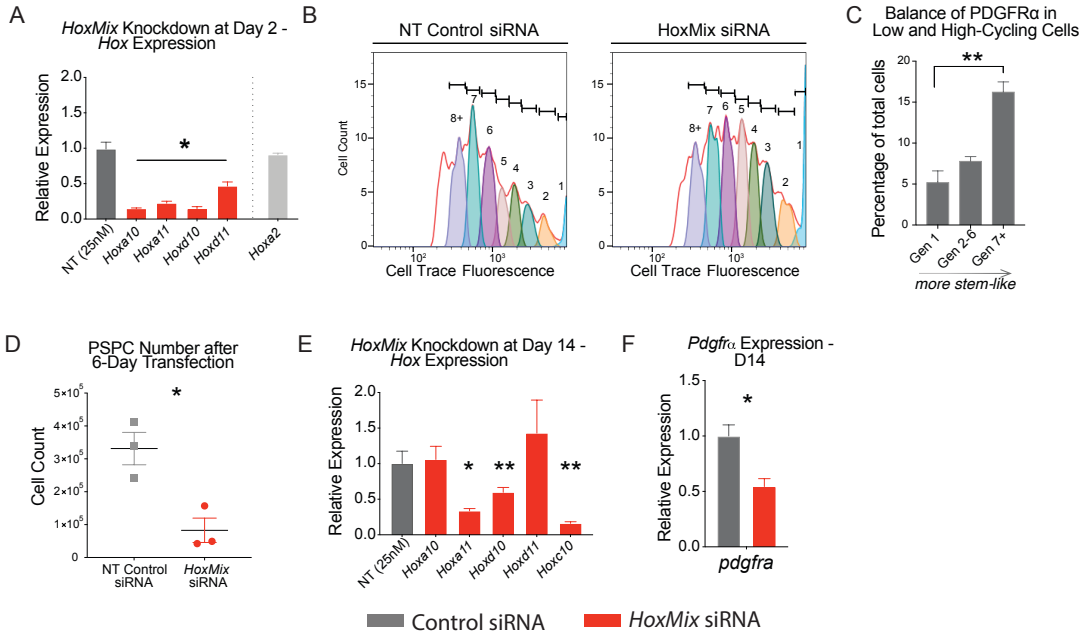

Supplementary Figure 2. Knockdown of posterior *Hox* genes in adult tibial PSPCs. (**A**) The expression of several posterior *Hox* genes in cultured PSPCs two days after knockdown with 5nM each of si*Hoxa10*, si*Hoxa11*, si*Hoxd10*, si*Hoxd11*, and si*Hoxc10* (termed *HoxMix* siRNA) normalized to their corresponding expression when PSPCs are transfected with non-targeting (NT) control siRNA (25nM). The expression of *Hoxa2* was used to ascertain specificity of the posterior *Hox* siRNAs. *n* = 3. (**B**) Representative cytometric plots of siControl- and si*HoxMix*-transfected tibial PSPCs that were treated with Cell Trace™ to categorize cells by cell cycle generation (from 1 to 8+) after six days of incubation. *n* =5 (control), *n* =7 (*HoxMix*). (**C**) The distribution of PSPCs displaying the skeletal stem cell marker, PDGFRα, among low-cycling (generation 1), medium-cycling (generation 2-6), and high-cycling (generation 7+) cells as measured by flow cytometry. (**D**) The absolute number of PSPCs after an equal seeding density and 6 days of transfection with either NT control or *HoxMix* siRNA. *n* = 3. (**E**) The expression of several posterior *Hox* genes in cultured PSPCs 14 days after a serial knockdown with 25nM of si*HoxMix* normalized to their corresponding expression in PSPCs transfected with 25nM NT control siRNA. *n* = 3. (**F**) qRT-PCR measured the relative gene expression of *pdgfr*α 14 days after a serial knockdown of PSPCs with si*HoxMix and* siControl. *n* = 3. **p* < 0.05, ***p* < 0.01. Two tailed Student's t-test. Error bars are SEM.

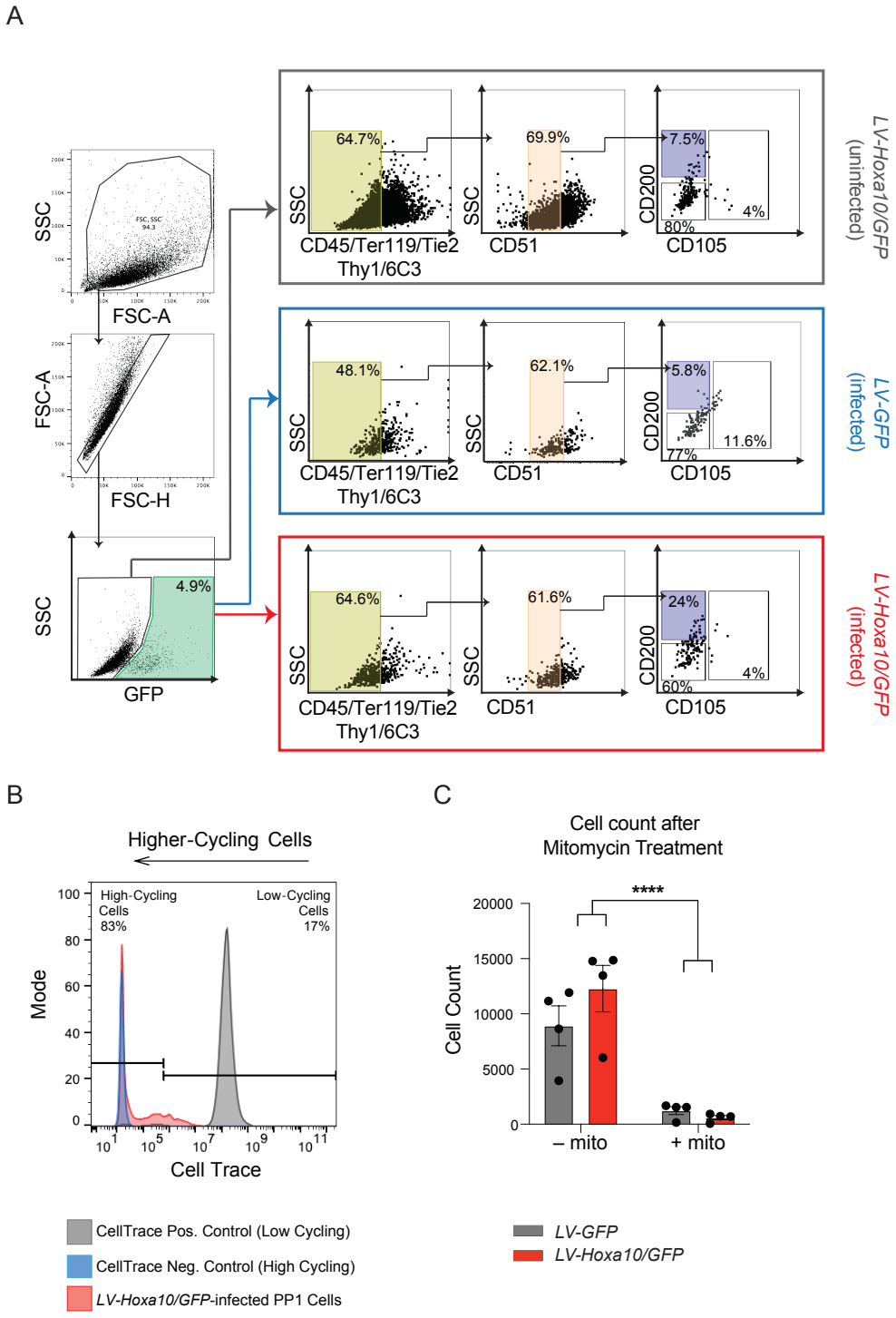

Supplementary Figure 3. Hoxa10 overexpression mediates reprogramming of adult tibial PP1 cells into PSCs. (**A**) Representative FACS plots of the PSPC lineage output 7 days after transduction of PP1 cells with *LV-GFP* or *LV-Hoxa10/GFP*. Infected (GFP^+) and uninfected (GFP^-) cells were evaluated separately. (**B**) Flow cytometric analysis on a CellTrace™ positive control (dye administration 30 minutes before analysis) and on a CellTrace™ negative control (no dye administration) was used to categorize cells as low- or high-cycling using the indicated gating strategy. A sample of *LV-Hoxa10/GFP*-infected PP1 cells after six days of *in vitro* administration of CellTrace™ was used as a representative sample. (**C**) The number of cells seven days after transduction of PP1 cells with LV-GFP or LV-Hoxa10/GFP with or without 10 μg/μl Mitomycin C treatment2. $n = 4$. ****$p < 0.0001$. Two tailed Student's t-test. Error bars are SEM.

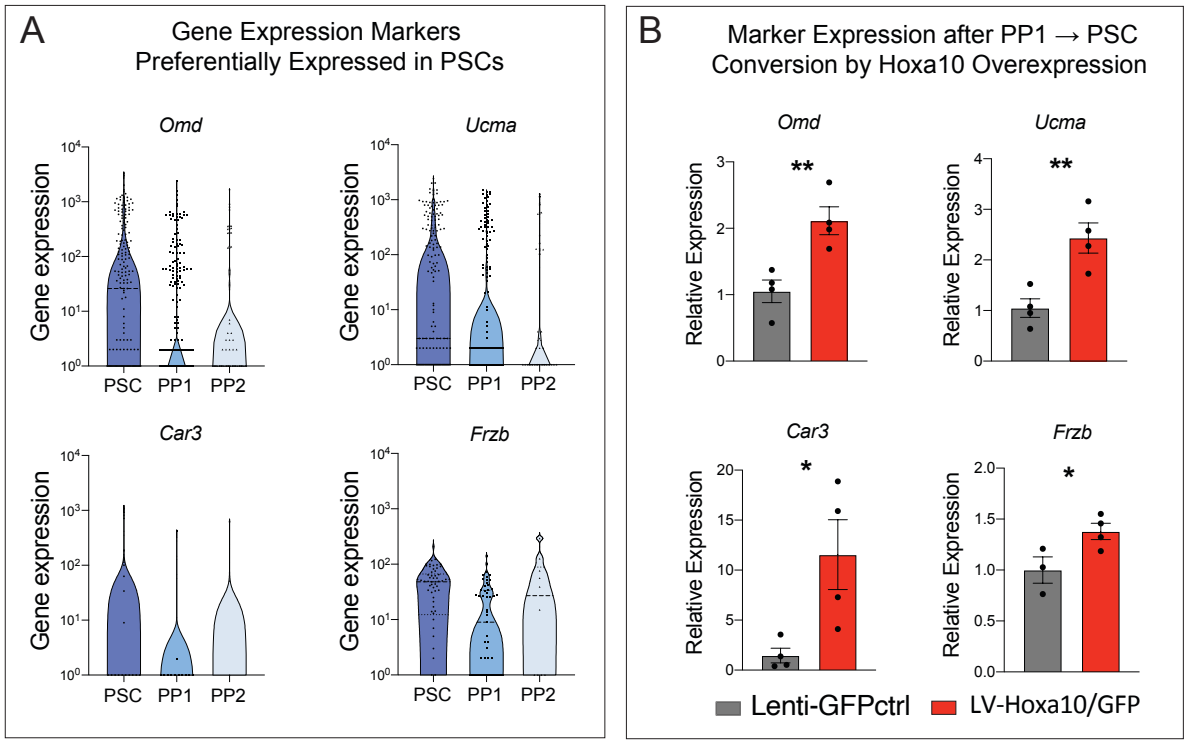

Supplementary Figure 4. Enriched periosteal stem cell marker expression after reprogramming of tibial progenitors. (**A**) Single-cell RNAseq data from Debnath, Yallowitz et al. 2018 was analyzed to obtain a list of marker genes that are enriched in PSCs relative to PP1 cells. PSC, PP1, and PP2 cells were sorted *in silico* based on genetic expression of CD51 (*itgav*), CD105 (*eng*), and CD200 (*cd200*) and on the gating strategy presented in Debnath, Yallowitz et al. 2018. n = 205 PSCs, n = 393 PP1 cells, n = 60 PP2 cells. (**B**) Relative gene expression of PP1 cells seven days after transduction with *LV-GFP* or *LV-Hoxa10/GFP* for the previously defined PSC markers. n = 4, *LV-GFP*; n = 4, *LV-Hoxa10/GFP.* *$p < 0.05$, **$p < 0.01$. Two tailed Student's t-test. Error bars are SEM.

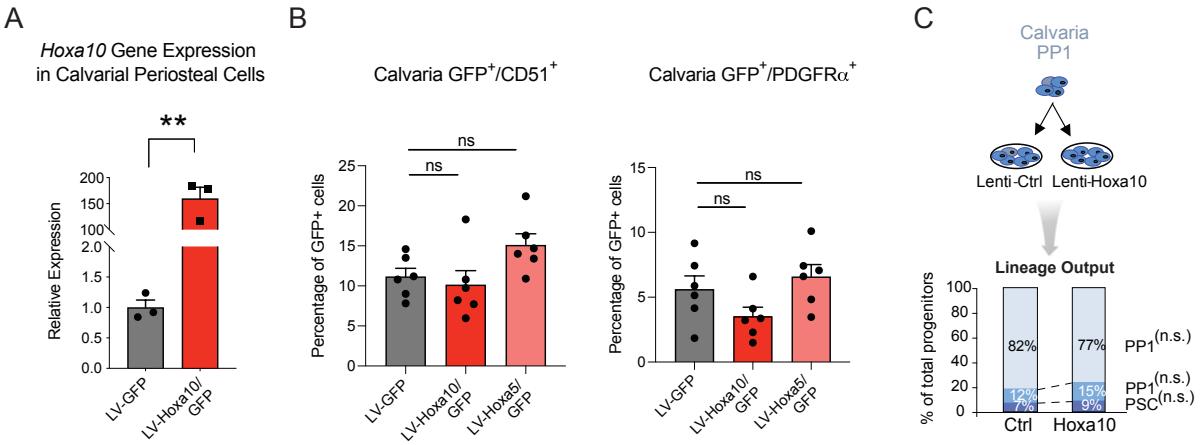

Supplementary Figure 5. *Hoxa10* overexpression in calvarial periosteal cells does not increase stem cell marker expression. (**A**) Relative expression of *Hoxa10* and *Pdgfrα* in calvarial PSPCs 6 days after infection with *LV-GFP* or *LV-Hoxa10/GFP,* as measured by qRT-PCR. *n* = 3, *LV-GFP*; *n* = 3, *LV-Hoxa10/GFP* (**B**) Seven days after transduction, flow cytometry revealed the balance of CD51$^+$, PDGFRα^+, or SCA1$^+$ stem cells among *LV-GFP*- or *LV-Hoxa10/GFP*-infected calvarial PSPCs. *n* = 3, *LV-GFP*; *n* = 2, *LV-Hoxa10/GFP. **p* < 0.01. Two tailed Student's t-test. Error bars are SEM.

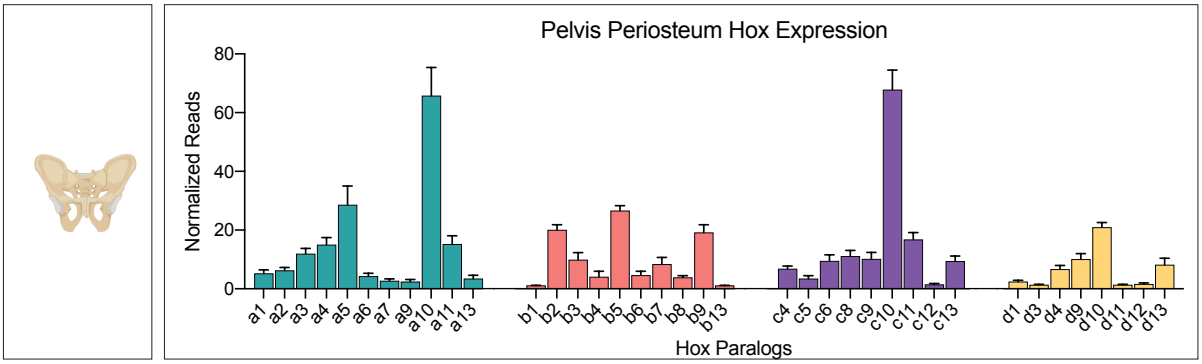

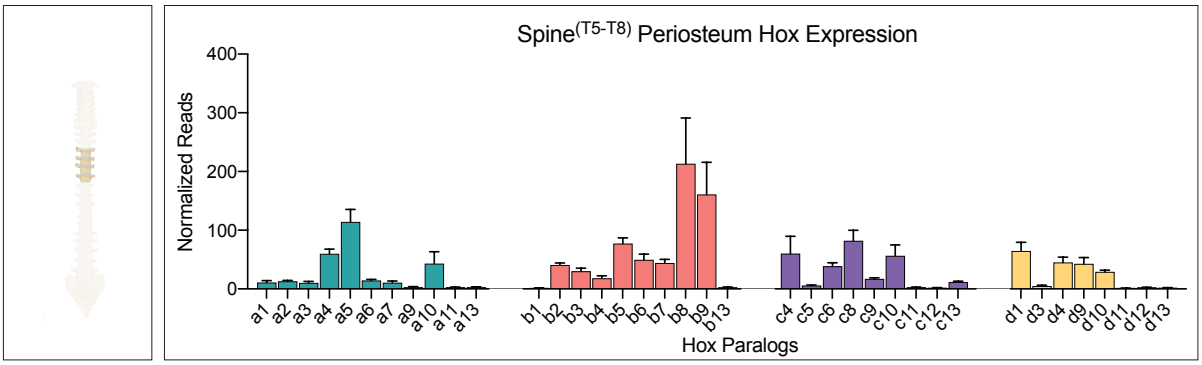

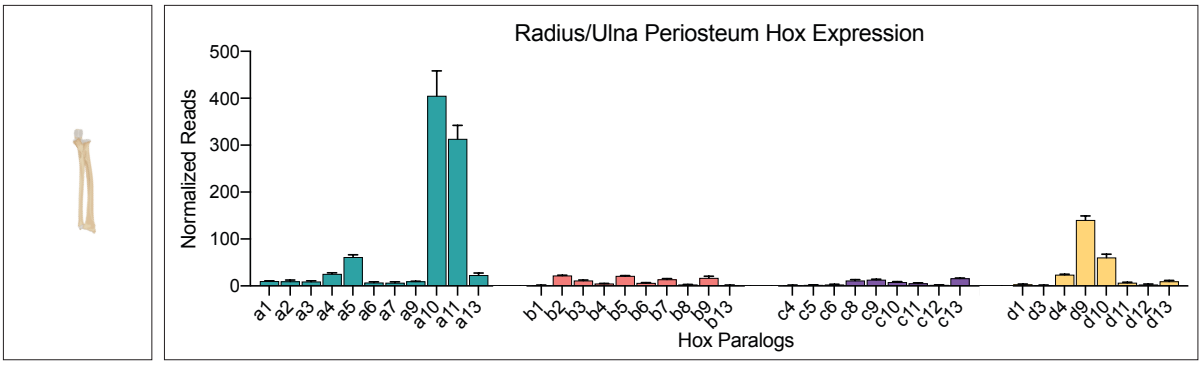

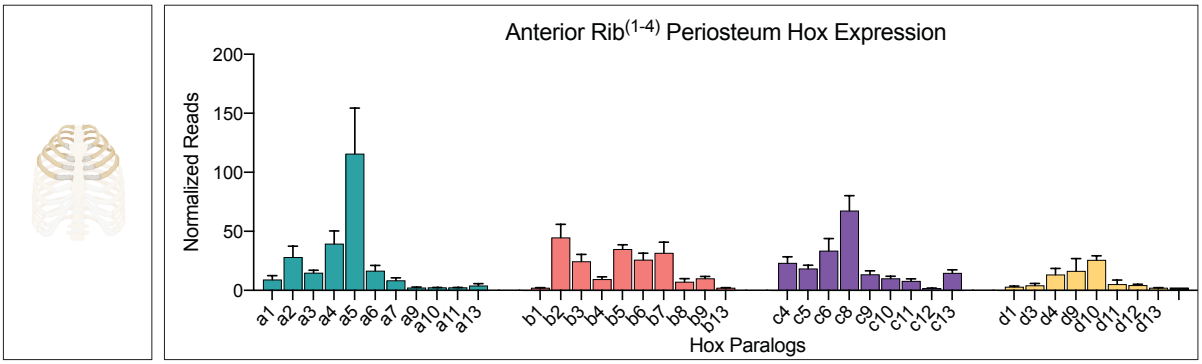

Supplementary Figure 6. *Hox* expression profile of 12-week-old periosteum from various anatomical regions. Nanostring^{TM} probes against all 39 Hox genes revealed their absolute expression profile in freshly-isolated periosteum of the pelvis, spine$^{T5\text{-}T8}$, radius/ulna, and anterior rib$^{1\text{-}4}$. *n* = 4 mice. Error bars are SEM.

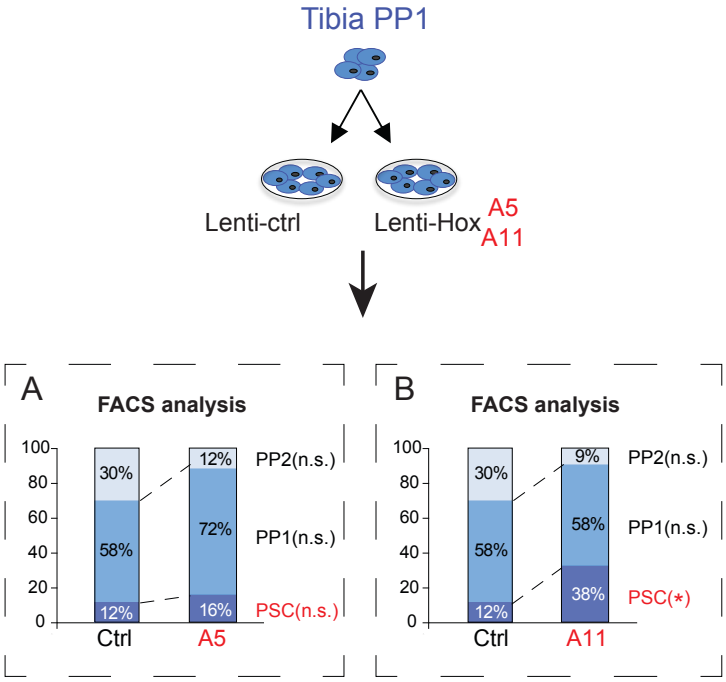

Supplementary Figure 7. Reprogramming of tibial periosteal progenitors is *Hox* code-dependent. (**A**) *Hoxa5*, an anterior *Hox* gene, does not change the lineage output of tibial progenitor cells 7 days after transduction with *LV-GFP* (Ctrl) or *LV-Hoxa5/GFP* (A5). (**B**) *Hoxa11* (adjacent to *Hoxa10*) shifts the lineage output of tibial progenitor cells 7 days after transduction with *LV-GFP* (Ctrl) or *LV-Hoxa11/GFP* (A11). Full lineage output data and statistics are provided in **Table 2.** *n.s.* = not significant, $*p < 0.05$. Two tailed Student's t-test.

Lineage Output

Infected Tibial Stem and Progenitor Cells

PSC

Exp.	PSC		PP1		PP2	
	Ctrl	Hoxa10	Ctrl	Hoxa10	Ctrl	Hoxa10
1	18.4% ±1.8 (n = 3)	16.6% ±2.0 (n = 3)	77.2% ±1.4 (n = 3)	77.6% ±2.0 (n = 3)	1.4% ±0.4 (n = 3)	2.9% ±0.2 (n = 3)
	p = 0.5291		p = 0.8653		p = 0.0957	

PP1

Exp.	PSC		PP1		PP2	
	Ctrl	Hoxa10	Ctrl	Hoxa10	Ctrl	Hoxa10
1	7.7% ±0.7 *(n = 3)*	15.5% ±1.5 *(n = 3)*	90.8% ±2.0 *(n = 3)*	81.7% ±1.9 *(n = 3)*	1.5% ±0.3 *(n = 3)*	2.8% ±0.4 *(n = 3)*
	p = 0.0172		*p = 0.0088*		*p = .0866*	
2	4.9% ±1.1 *(n = 3)*	15.7% ±1.1 *(n = 3)*	92.0% ±1.1 *(n = 3)*	77.4% ±2.4 *(n = 3)*	0.2% ±0.2 *(n = 3)*	1.4% ±0.6 *(n = 3)*
	p = 0.0020		*p = 0.0053*		*p = 0.1209*	
3	14.9% ±0.5 *(n = 4)*	18.9% ±1.0 *(n = 4)*	80.5% ±0.6 *(n = 4)*	74.5% ±1.3 *(n = 4)*	2.2% ±0.2 *(n = 4)*	3.3% ±0.4 *(n = 4)*
	p = 0.0120		*p = 0.0064*		*p = .0529*	
4	8.9% ±1.0 *(n = 3)*	21.4% ±3.1 *(n = 4)*	90.3% ±0.9 *(n = 3)*	76.3% ±3.0 *(n = 4)*	0.6% ±0.3 *(n = 3)*	1.1% ±0.2 *(n = 4)*
	p = 0.0078		*p = 0.0044*		*p = .1245*	
5	11.6% ±5.1 *(n = 5)*	52.4% ±10.9 *(n = 6)*	58.2% ±17.7 *(n = 5)*	39.4% ±9.9 *(n = 6)*	30.2% ±18.8 *(n = 5)*	9.5% ±5.3 *(n = 6)*
	p = 0.0114		*p = 0.3578*		*p = 0.2787*	
+ mito	3.7% ±3.7 *(n = 3)*	28.0% ±6.9 *(n = 3)*	92.1% ±4.0 *(n = 3)*	57.7% ±7.5 *(n = 3)*	4.2% ±4.2 *(n = 3)*	14.3% ±14.3 *(n = 3)*
	p = 0.0362		*p = 0.0152*		*p = .5336*	

PP2

Exp.	PSC		PP1		PP2	
	Ctrl	Hoxa10	Ctrl	Hoxa10	Ctrl	Hoxa10
1	32.6% ±6.5 *(n = 3)*	20.6% ±2.9 *(n = 3)*	15.1% ±5.1 *(n = 3)*	12.3% ±1.5 *(n = 3)*	52.2% ±3.5 *(n = 3)*	67.1% ±3.2 *(n = 3)*
	p = 0.2328		*p = 0.5952*		*p = 0.4928*	
2	0.37% ±0.04 *(n = 5)*	0.44% ±.01 *(n = 5)*	8.3% ±0.8 *(n = 5)*	6.9% ±0.7 *(n = 5)*	89.1% ±1.2 *(n = 5)*	91.2% ±0.7 *(n = 5)*
	p = 0.6017		*p = 0.2349*		*p = 0.1606*	

Table 1. The lineage output after *Hoxa10* overexpression in adult tibial PSPCs. The lineage hierarchy of sorted PSCs, PP1 or PP2 cells was evaluated by flow cytometry seven days after transduction with *LV-GFP* (Ctrl) or *LV-Hoxa10* (Hoxa10). Only infected GFP$^+$ cells were assessed. Multiple separate experiments (Exp.) are shown.

Lineage Output

Infected Periosteal Progenitors

Tibia PP1

Hox	PSC		PP1		PP2	
	Ctrl	Hox	Ctrl	Hox	Ctrl	Hox
A5	11.6% ±5.1 (n = 5)	15.8% ±3.9 (n = 6)	58.2% ±17.7 (n = 5)	72.4% ±4.7 (n = 6)	30.2% ±18.8 (n = 5)	11.8% ±1.4 (n = 6)
	p = 0.5299		p = 0.4185		p = 0.3078	
A11	11.6% ±5.1 (n = 5)	32.4% ±5.7 (n = 6)	58.2% ±17.7 (n = 5)	58.2% ±6.9 (n = 6)	30.2% ±18.8 (n = 5)	9.4% ±2.7 (n = 6)
	p = 0.0260		p = 0.9982		p = 0.2573	

Spine^{T5-8} PP1

Hox	PSC		PP1		PP2	
	Ctrl	Hox	Ctrl	Hox	Ctrl	Hox
A10	12.9% ±1.7 (n = 3)	16.7% ±2.7 (n = 3)	79.0% ±4.1 (n = 3)	75.7% ±1.6 (n = 3)	4.2% ±2.1 (n = 3)	6.6% ±0.4 (n = 3)
	p = 0.2994		p = 0.4950		p = .3695	
B8	14.9% ±1.3 (n = 4)	24.6% ±4.0 (n = 4)	80.7% ±2.1 (n = 4)	67.5% ±4.3 (n = 4)	5.4% ±1.1 (n = 4)	7.9% ±0.7 (n = 4)
	p = 0.0435		p = 0.0338		p = 0.0964	
B8	12.3% ±3.3 (n = 4)	31.8% ±5.5 (n = 4)	60.2% ±8.2 (n = 4)	48.9% ±7.1 (n = 4)	25.5% ±10.9 (n = 4)	19.4% ±1.6 (n = 4)
	p = 0.0120		p = 0.0064		p = .0529	

Ant. Rib$^{1-4}$ PP1

Hox	PSC		PP1		PP2	
	Ctrl	Hox	Ctrl	Hox	Ctrl	Hox
A10	10.2% ±0.5 (n = 6)	12.5% ±2.7 (n = 6)	80.4% ±2.3 (n = 6)	83.4% ±3.3 (n = 6)	9.4% ±2.1 (n = 6)	3.1% ±1.4 (n = 6)
	p = 0.0606		p = 0.5727		p = 0.3189	
A10	5.7% ±2.8 (n = 9)	8.9% ±3.5 (n = 9)	64.5% ±11.3 (n = 9)	59.5% ±10.9 (n = 9)	29.8% ±11.8 (n = 9)	31.6% ±12.7 (n = 9)
	p = 0.4824		p = 0.7528		p = 0.9168	
A5	5.7% ±2.8 (n = 9)	15.4% ±2.5 (n = 8)	64.5% ±11.3 (n = 9)	73.1% ±4.0 (n = 8)	29.8% ±11.8 (n = 9)	11.6% ±2.5 (n = 8)
	p = 0.0218		p = 0.4875		p = 0.1504	

R/U PP1

Hox	PSC		PP1		PP2	
	Ctrl	Hox	Ctrl	Hox	Ctrl	Hox
A10	13.3% ±5.3 (n = 5)	15.3% ±1.8 (n = 5)	83.3% ±4.3 (n = 5)	76.0% ±2.4 (n = 5)	3.4% ±1.2 (n = 5)	8.3% ±1.3 (n = 5)
	p = 0.7350		p = 0.1746		p = 0.0253	
A11	8.3% ±5.3 (n = 5)	37.5% ±1.1 (n = 4)	37.8% ±8.3 (n = 5)	22.5% ±3.4 (n = 4)	56.0% ±2.4 (n = 5)	40% ±11.2 (n = 4)
	p = 0.01967		p = 0.2481		p = 0.222	

Pelvis PP1

Hox	PSC		PP1		PP2	
	Ctrl	Hox	Ctrl	Hox	Ctrl	Hox
A11	6.1% ±1.8 (n = 5)	24.6% ±4.2 (n = 5)	65.2% ±14.7 (n = 5)	65.5% ±3.6 (n = 5)	26.4% ±12.8 (n = 5)	9.6% ±1.8 (n = 5)
	p = 0.7350		p = 0.1746		p = 0.0253	

Table 2. The lineage output after *Hox* overexpression in adult PSPCs from various anatomical regions. The lineage hierarchy of sorted PSCs, PP1 or PP2 cells was evaluated by flow cytometry seven days after transduction with *LV-GFP* (Ctrl), *LV-Hoxa10* (Hoxa10), or a lentivirus containing the Hox gene shown to have the highest expression in each corresponding skeletal element. Only infected GFP^+ cells were assessed. Multiple separate experiments are shown.

Gene	Oligonucleotide Probe
Hoxa1	ACGTCTTCTCCAGCGCAGACCTTTGACTGGATGAAAGTTAAAAGAAACCCTCCCAAAACAGGGAA AGTTGGAGAGTACGGCTACGTGGGTCAACCCAACG
Hoxa10	AACCGAGAAAACCGAATCCGGGAGCTCACAGCCAACTTTAATTTTTCCTGATGAAACTTCCAGAC AACGTCTTTTCGCTTCCTGAGCGCCTGGACCCATC
Hoxa11	GGTTACAGTACTACTCAGCTAATCCACTTCTCTAAGGCTCCAGCCTACTGGAATTGGGAGGGGG GCTTCATACATGTGAAATAATATGCAGATTTTGCCC
Hoxa13	GCCTTACACTAAGGTGCAGTTGAAAGAACTCGAACGGGAATACGCTACGAACAAATTCATTACCA AGGACAAACGGAGGAGGATATCAGCCACGACAAAC
Hoxa2	AGGGTACACTTTTCAGCAAAATGCGCTCTCTCAACAGCAGGCTCCCAATGGACACAATGGCGACT CCCAAACTTTCCCAGTTTCGCCTTTAACCAGCAAT
Hoxa3	ATGGGACCCCACACTTACAGGGAAGCCCCGTCTTCGTAGGGGGCAGCTATGTGGAGCCCATGA GCAACTCTGGGCCACTCTTTGGCCTAACTCACCTCCC
Hoxa4	TAGAGACCTGGATCAGTTTCTCTCACTTATGTGCCCTACTCATCTCCTGCTCCTGTCCTCATCTGC TCTTCCCTAAGTAAACCCGAGACACCAAAACAAA
Hoxa5	GAGGTGACTTGATAAGACACAAATTAACTTGTTCAACGTGTAGTGGCTAGTGGCTCTGTGACGAA AACTGTGACTCCAAGCGGTGTGTCCCTGCGTGCCT
Hoxa6	CCTTCCCGGCCTCTTACGGGGCGTCGAGTCTTCCGGACAAGACATACACCTCACCTTGTTTTTAC CAACAGTCCAACTCGGTCTTGGCCTGCAACCGGGC
Hoxa7	GCTTTTATTGTCTCCTAAAGAACTGGGGTTCCACAATGAGCTACAGCACCCAGGTCCTGAGATTA CCTCTCCTGTCTCTAATCCAGCTCTAAAACTGTTA
Hoxa9	ATCGTGGAGCTGCGCGATCCCTTTGCATAAAAACATATGGCTTTTGCTATAAAAATTATGACTGCA AAACACCGGGCCATTAATAGCGTGCGGAGTGATT
Hoxb1	CCTCTTGAATTGAACTTCCTAAGTAACTGGGCTTCCAACGCTTGACCAGTTCTCTCGAAGACTTTC CCAAACTTCACAGCCTTGGTGACCCTCCTCAAGG
Hoxb13	CGCCGAGGCCGCAAAAAACGCATTCCCTATAGCAAGGGGCAGTTGCGGGAGTTGGAGCGGGAG TATGCAGCCAACAAGTTTATCACTAAGGACAAGAGGC
Hoxb2	GACTTCTTCACCAGCACGCTCTGTGCCATCGACTTGCAGTTTCCCTAACTGTTTTCCATCTTTGGT CCTTTCCGTCTGGTCCTCCTTGGCTGTTGGGGGC
Hoxb3	GCCAGGGAGACGGCGGACTTGGGGGATGGGCGCGGTTTAGAGTCCTGAAAGAGGTGTGGGAT GGGGTTGTCGCCAGGTTTCCAGAAACAGAACAGGCCTG
Hoxb4	GTAGGGTCCGGGTGAGCAGATTTCCTTATCCGGGAATCGCAGGCCGGGTGGCCATTGGCTCGG AGGATCACGTGGGCCTCTAACTTTGTTCACTTGACAG
Hoxb5	GTCAGGCCAATCACTTCCTCTCTCACCCATTTCGCTTCCAAGACCATTTGTAGTGAGCGGGTGGA TGCTGTGCTACGTGTGAAATCTGTCTTTGCCAGGC
Hoxb6	CTCATCAGGCTCTCTGGTGAGAACTGAGAATCGGACTCACTTGATGTCTCCTGGAAGCAGAGCA GAATGCTCATGTCCTTGTCGAGTCTCATTTCGTCCA
Hoxb7	GATCCACTAGCTTCTGCGTCTGGTGCATTTTGGCTGCTGTTTCTAGGTCCTATTCACGAGCCTCTT TCTGTATATCTGAAGGATGGAAAATAAAACAGGA
Hoxb8	AGACGGGGCAAAATATGAAACAACTCATTTGGAGGGAAGTAAATCACCGAAAACTGTTTATGAAC TGGCATCCCTTCTTCGAAATGTAAAGCGAGGACCT
Hoxb9	CCACAGACATAGAGTTTGGAGTCTATGCTAATCATCGTGGAGAAAGGACATCAAGACGTTGTTCA TCAAACCAAGCAGGGCAGCTCTCAGATCAGGTTCA
Hoxc10	GTGTGTGTGTCAACTCTTCAGTCACCCATGCACTCACATACAGCATTCTGTTCTCCATGCAAAGTT GAGGTCAAATGCACCCGATTAGAGGGGAAAGAAA
Hoxc11	TCCCGGATGCTGAACCTGACAGACCGACAAGTGAAAATTTGGTTTCAGAACAGGAGAATGAAAGA AAAAAAACTGAGCAGAGACCGGCTGCAGTATTTTT
Hoxc12	AGCATAATCTCCTGAATCCTGGGTTTGTGGGGCCGCTGGTGAATATCCACACAGGAGACACCTTC TACTTCCCCAACTTCCGCGCGTCAGGGGCACAACT
Hoxc13	CGCCCGTCCCGACTATTTATGTCACAGCTTTGTACCATAACGGAATCCACCCGAAGGACGCTGCA CCGGCGCAGACCACTATTTAATCTTACCGAGAAAG
Hoxc4	TTTGAATAAAGCGATTCGGTTCCTTATCCGGGGACTGGGTTGCTCGGTGTGATTGGCCGGCGGA GTCACATGGTGAAAGTAACTTTACAGGGTCGCTAGC
Hoxc5	CTGAGTTCTTTTCTTGATTCATGGTTCCAAGAAGGGCCTCTGGGGTGAAGGGGAGTACACTTGAG GACTCCTGTACTGTTGTTTCCACTTGCTGTGTGTG
Hoxc6	AGCTCAGAACCGGATCTACTCGACTCCCTTTTATTCGCCACAGGAGAATGTCGTGTTCAGTTCCA GCCGGGGGCCGTATGACTATGGATCTAATTCCTTT
Hoxc8	CCCAGACAGTCCCTTTATGGGGCTCAGCAAGAGGCGAGCGTGGTGCAATATCCCGACTGTAAAT CCTCCGCCAACACTAACAGTAGCGAAGGACAAGGCC

Hoxc9	GCAAATTTCCTTGCGATACATACATCACACAAAAGATCAGAGACTGCAGGAGCGTCGGAGCCGA CAGAGACAGATTACGTCAAGAAATAGTTCCTCCACC
Hoxd1	TTAGCTACCTGCCTAAACGCTGCTATGTGAGCCACTTAAAATTCTCGGGTGCAGAGTGGCAGGCC TTCTTAGTCTAGTGTGGTCAGAAACGTATCTCTCT
Hoxd10	CCTTGTGGTGCATCTGTGGTTTGGTAGAAGTACAAGCGCAACCTGTGCTTTTCTGTGCATGTTCT GGTCGCATGTGTAATGCAATAAACTCTGGAAATGG
Hoxd11	TTAAGAAGAAGAAGGGGGTAAAATCCTCCTTGTGAGGCGGGGGAAGTTTGTTAAGAGGAAGTTA ATAGGTGCAGGGACTTGGGGTCTTTCTGATGTCATG
Hoxd12	AAACATTCAGCATGGTGTCTGGGGGTCACCTGTCCTTGTCTATGATGTTTACATCCGGGGCTCAC TATTGAAACACTGTATGAGGGTTTGTTTTTTCCGG
Hoxd13	GGATCTCAGCTGCCACGAACCTTTCGGAGAGACAAGTAACCATTTGGTTTCAGAATCGAAGGGTG AAGGACAAGAAAATCGTCTCCAAGCTCAAAGACAC
Hoxd3	TCGCACACATCTGCAAGCAGATCACTCTGTCTTCATCCCTCTGTATGATCCCGGGTTGGGGGAAA AGGACCCTCTGAAACATTTTATTTATTCGGAACCT
Hoxd4	GGGCGGGCTTCTTTAAGTAGATTATCATATGGCAGGAGCTACTGAGAACATAAACCCTTGGCGAG TCATTAAACTCCTGAAAATCTCTGCTGGTGGATTG
Hoxd8	TACTGGTGGACACCACCGGTCCTCCCTCTTGTGTTTTGGAAACGGACTTTACCTGTGTTTCAAGC TACCTTAATGTCACTGCTCTTGAGGTTTCTGCGCT
Hoxd9	TTTTTAGGTAGAAGTGACTGTGTGGTTGGTCTCTGTGAGTTATCTGGGGGACACTGTATTTGCTC GCATATGTATTGGAGAAACCAAGTGGCTTTGGAGT
PGK1	CCGGCATTCTGCACGCTTCAAAAGCGCACGTCTGCCGCGCTGTTCTCCTCTTCCTCATCTCCGG GCCTTTCGACCTCACGGTGTTGCCAAAATGTCGCTT
TBP	GTGGCGGGTATCTGCTGGCGGTTTGGCTAGGTTTCTGCGGTCGCGTCATTTTCTCCGCAGTGCC CAGCATCACTATTTCATGGTGTGTGAAGATAACCCA
TUBB	ATTGGAAGTGTCTTCCCTGTATTGGTTCTCCTTTCTCGGAGAGATGGGGGTTGGGGGTGCGGCA AGGTCTTGGTCTTGGTCTCTGAACACTCCCAATTCC
ACTB	CAGGTCATCACTATTGGCAACGAGCGGTTCCGATGCCCTGAGGCTCTTTTCCAGCCTTCCTTCTT GGGTATGGAATCCTGTGGCATCCATGAAACTACAT
GUSB	CCCTTCGGGACTTTATTGGCTGGGTGTGGTATGAACGGGAAGCAATCCTGCCACGGCGATGGAC CCAAGATACCGACATGAGAGTGGTGTTGAGGATCAA

Table 3. Nanostring™ Custom Hox CodeSet. Oligonucleotides probes generated for the 39 Hox genes and 5 housekeeping genes used to probe absolute gene expression.

Primer Name	Sequence (5'-3')
18s FOR	ACGAGACTCTGGCATGCTAACTAGT
18s REV	CGCCACTTGTCCCTCTAAGAA
Car3 FOR	CCACAATGGTCCTGATCAC
Car3 REV	TTAGTATGCAGTTCAATGGGTG
Col2a1 FOR	TCCAGATGACTTTCCTCCGTCTA
Col2a1 REV	CAGGTAGGCGATGCTGTTCTTAC
Cyclind1 FOR	TCCCAGACGTTCAGAACC
CyclinD1 REV	AGGGCATCTGTAAATACACT
Fabp4 FOR	AAGAAGTGGGAGTGGGCTTT
Fabp4 REV	AATCCCCATTTACGCTGATG
Fosb FOR	GATCGCCGAGCTGCAAAAAG
Fosb REV	CCTTAGCGGATGTTGACCCTGG
Foxo1 FOR	TACGAGTGGATGGTGAAGAG
Foxo1 REV	AATTGAATTCTTCCAGCCCG
Frzb FOR	CCTCTGTCCTCCACTTACTG
Frzb REV	ACCAAGAGTAACCTGGAACG
Hoxa10 FOR	TTCGCCGGAGAAGGACTC
Hoxa10 REV	TCTTTGCTGTGAGCCAGTTG
Hoxa11 FOR	TTTGATGAGCGTGGTCCCTG
Hoxa11 REV	AGGAGTAGGAGTATGTCATTGGG
Hoxa2 FOR	GTCACTCTTTGAGCAAGCCC
Hoxa2 REV	TAGGCCAGCTCCACAGTTCT
Hoxc10 FOR	CCTCGCAATGTAACTCCGAACT
Hoxc10 REV	ACCCCGCAATTGAAGTCACT
Hoxd10 FOR	GGAGCCCACTAAAGTCTCCC
Hoxd10 REV	TTTCCTTCTCCTGCACTTCG
Hoxd11 FOR	ACACCAAGTACCAGATCCGC
Hoxd11 REV	AGTGAGGTTGAGCATCCGAG
Oc FOR	TGTGACGAGCTATCAAACCAG
Oc REV	GAGGATCAAGTTCTGGAGAGC
Omd FOR	CCAAGGAATTTGGAACATCTATACC
Omd REV	GGAGAAGGACATATCATTGTCAC
Osx FOR	GGAGACCTTGCTCGTAGATTTC
Osx REV	GGGATCTTAGTGACTGCCTAAC
Pdgfrα FOR	AGAGTTACACGTTTGAGCTGTC
Pdgfrα REV	GTCCCTCCACGGTACTCCT
Ppar-γ FOR	ATAGGTGTGATCTTAACTGCCG
Ppar-γ REV	CCAACAGCTTCTCCTTCTCG
Runx2 FOR	CGGTCTCCTTCCAGGATGGT
Runx2 REV	GCTTCCGTCAGCGTCAACA
Sox9 FOR	TACGACTGGACGCTGGTGC
Sox9 REV	TTCATGGGTCGCTTGACGT
Ucma FOR	CGAGATGAAGTTAATGCGGA
Ucma REV	AAACTCGTTCCTTTGCTCC

Table 4. qRT-PCR primers. All primers were purchased from Integrated DNA Technologies.